King Fahd University of Petroleum and Minerals

Aerospace Engineering Department

Aerospace System Design

(AE 427)

Term Project

Done By:

Category	Major	Minor
Project leadership	**Salman AL-Fifi**	Ghassan Gawwas
Aerodynamics	Uthman Mushari	Ali Abatahin
Propulsion systems	Abdullah Barrak	Ghassan Gawwas
Performance & stability	Khaled AL-Anazi	Salman AL-Fifi
Weight & balance & Structures	Mohammed Nwaser	Abdullah Barrak
Advance technology	Mohammed Nwaser	Ali Abatahin
Computer Graphics	Ghassan Gawwas	Uthman Mushari
Market survey & cost analysis	Ali Abatahin	

1. Background

1.1 Overview: (Ref. 1)

"Entering the new millennium, we find ourselves in the midst of the third major evolutionary stage of the regional air transport industry, the most dynamic and exciting sector in air transportation today. The first major development was, of course, marked by the passage of the United States' Airline Deregulation Act of 1978. In due course this has been followed by similar legislation in most other countries of the world, most notably in the liberalization and deregulation that has taken place in Europe over the past few years. We can safely say that the liberalization of aviation market places is now global in its reach, most recently establishing itself in the People's Republic of China.

The 1980s and early 1990s have been marked by exceptional growth in the regional airline industry. In 1982, manufacturers took orders for 107 turboprops of between 20 and 99 seats; by 1989 orders had grown to more than 511 turboprops. World regional passenger traffic grew from a little more than 50 million passengers in 1987 to almost 230 million passengers today. In the 1980s, the speed and effective service area that was available through first generation turboprop technology limited regional airline's ability to expand their reach into new markets.

In response to these limitations, aircraft manufacturers, in 1992, introduced a new type of regional aircraft. This marked what is regarded as the second stage of development of the regional airline: for the first time, regional airlines had the option of a cost effective 50-seat jet aircraft with which to pursue new markets and rationalize service in existing ones.

We now come to the new millennium. What will be the shape of regional air transportation? In the new millennium, we know that passenger expectations are higher, the service bar has been raised, and the differences between "regional" and "mainline" airlines have blurred: the "seamless" service that airline alliances are promising will lead to demands for 'equivalent-to-mainline services' regardless of aircraft type; what is delivered on one segment of a flight will be expected on all segments. Air traffic congestion will increase in the short-term, access to airport slots will become increasingly constrained and the volatility of fuel prices will remain an unpredictable factor influencing the cost of air travel. Noise and emission issues are taking on increasing international significance and will have impact on fleet planning and the next generation of aircraft design

In response to increased regional enplanements, and system-wide congestion, the airline industry has already started to move toward the purchase of larger, more efficient regional aircraft, both jets and turboprops.

This Regional Market Outlook 2001 forecast reflects many of these developments through the trend toward more and larger regional aircraft. While the early part of the forecast emphasizes the growth in the 50-seat market, the later part suggests that in the absence of labour and other restrictions, the 50-seat market will be supplemented and perhaps supplanted by demand for larger 70-seat aircraft

The expectation from airlines is for manufacturers to provide a family of aircraft that will offer flexible and cost-saving operations through common crewing, maintenance, spares and after-sales support. So, we led the way in this regard, developing a new technology of 80 to 100-seat aircraft. Aircraft such as these will continue to be developed to meet the

needs and demands of passengers and airlines in all over the world," especially in Saudi Arabia.

1.2 Market survey:

According to ref.1, the regional airline industry is strong with deliveries of 8,345 aircraft forecast for the next twenty years. Almost two-thirds of all deliveries will occur in the US and Europe.

Deliveries will be strongest for the 50-seat regional aircraft at the onset of the forecast period and will gradually shift toward favoring 70 and 90 seat aircraft.

• Sustained economic growth: The US economy, which is a key driver of global economic activity, has displayed exceptional strength into the new millennium while currently experiencing a downturn, long-term 20-year GDP growth is expected to be strong and positively affect air traffic demand

• Regional airline industry phenomenal growth to continue: The regional aircraft market continues to be a key growth sector of the airline industry. More than 200 million passengers world-wide enplaned regional aircraft last year

The regional aircraft fleet will double in the next twenty years with expected revenues for the 20-99 seat aircraft deliveries to be $183 billion US in 2000 dollars.

• Trend toward larger, more efficient regional jets and turboprops: The smallest regional aircraft seat category, 20-39 seats, will see delivery of 11% of all aircraft, while almost half (45%) of all deliveries will be in the 40-59 seat category. The 60-79 seat range will capture just under one-third (33%) of all deliveries. The 80-99 seat category is expected to complete the picture with another 11% of all forecast deliveries.

1.2.1 Worldwide Aircraft Deliveries

All Markets, 20-99 Seats, 2001-2020:

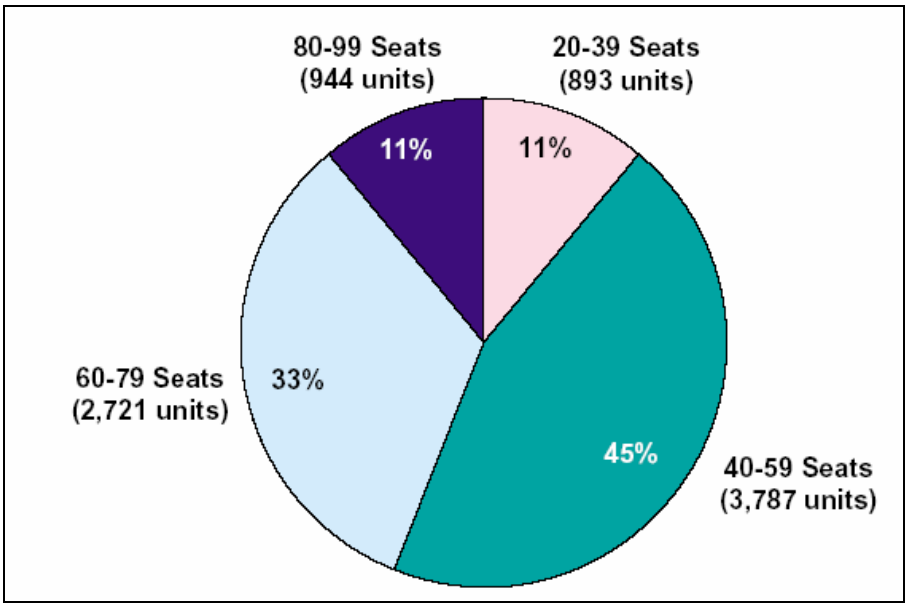

Figure 2.1 Aircraft delivers of 20-99 seat from 2001 to 2020
(Total Deliveries = 8,345)

1.2.2 Worldwide Regional Aircraft Forecast

20 - 99 Seats, Deliveries and Revenues 2001 – 2020:

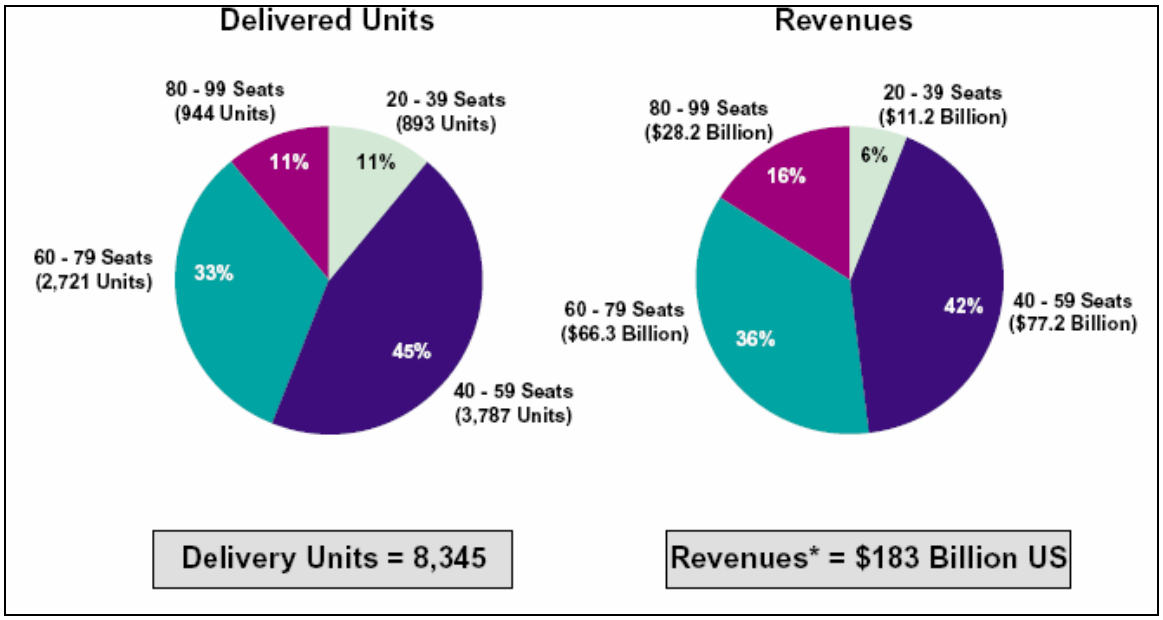

Figure 2.2 Regional Aircraft Forecast 20 - 99 Seats, Deliveries and Revenues 2001-2020

1.2.3 Worldwide Aircraft Delivery Forecast

20 - 99 Seats, 2001 - 2020

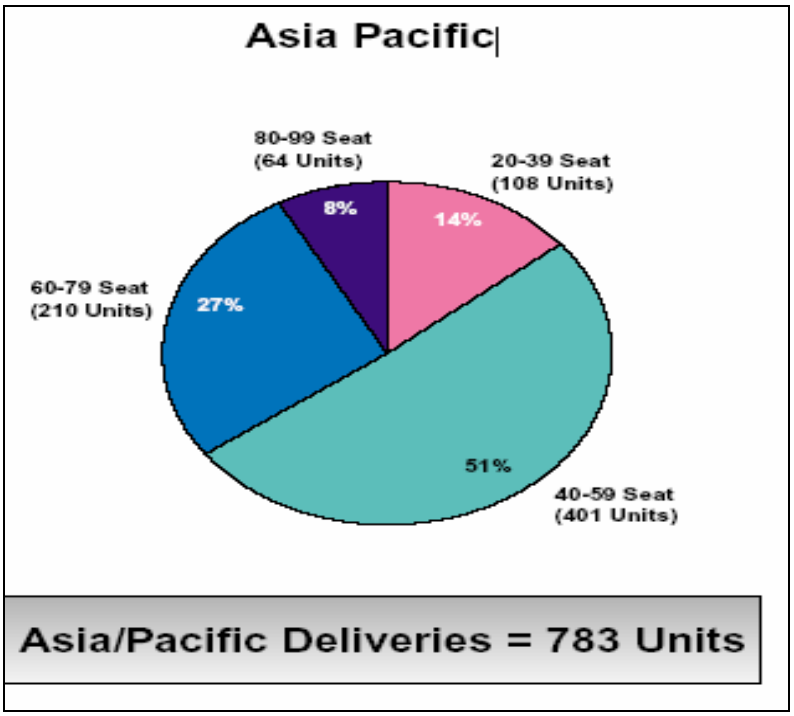

Figure 2.3 20 - 99 Seats, 2001 – 2020

1.2.4 Worldwide Delivery Forecast

Turboprop-Jet Split-20-99 Seats, 2001-2020

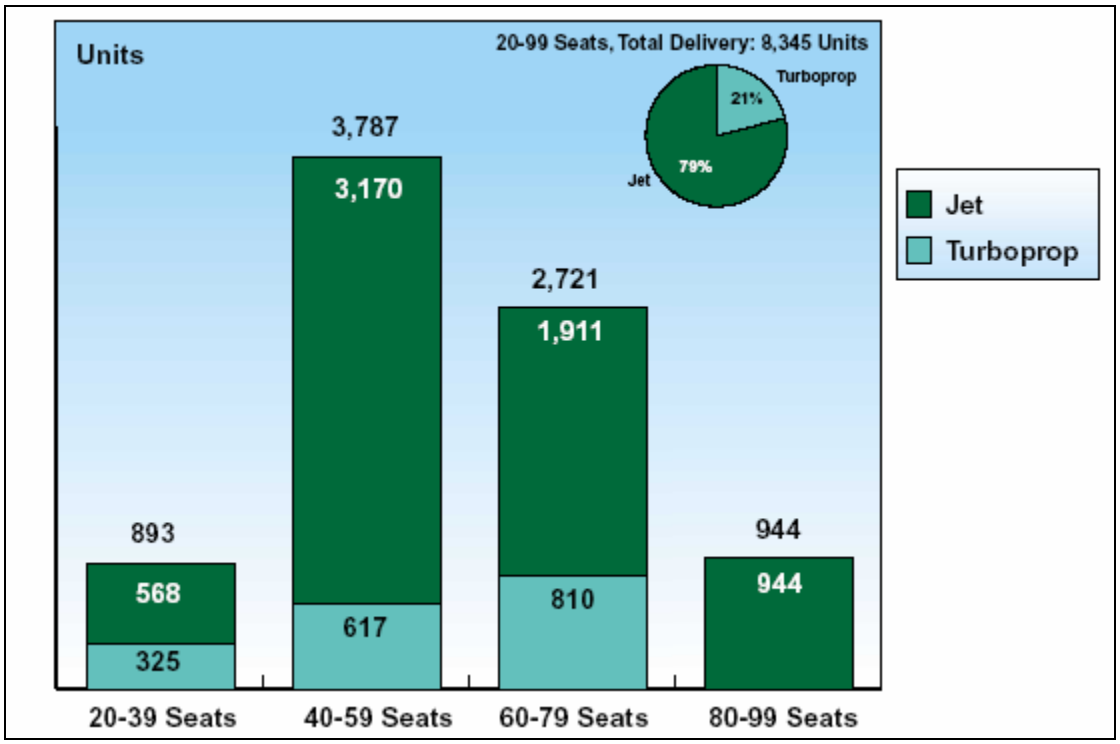

Figure 2.4 Turboprop-Jet Split 20 - 99 Seats, 2001 – 2020

1.2.5 Worldwide Regional Aircraft Fleet Forecast

All Markets, 20 - 99 Seats:

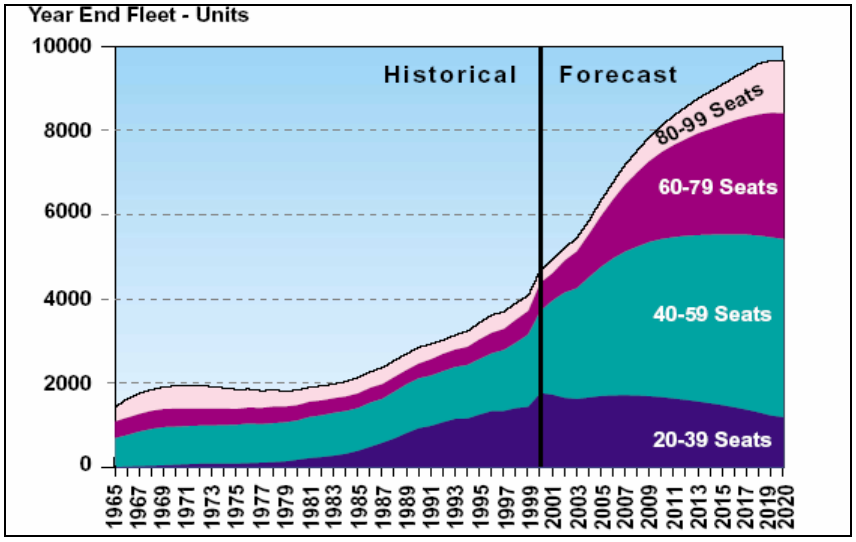

Figure 2.5 Worldwide Regional Aircraft Fleet Forecast 20 - 99 Seat

1.2.6 Regional routes in Saudi Arabia and gulf region (Ref. 3):

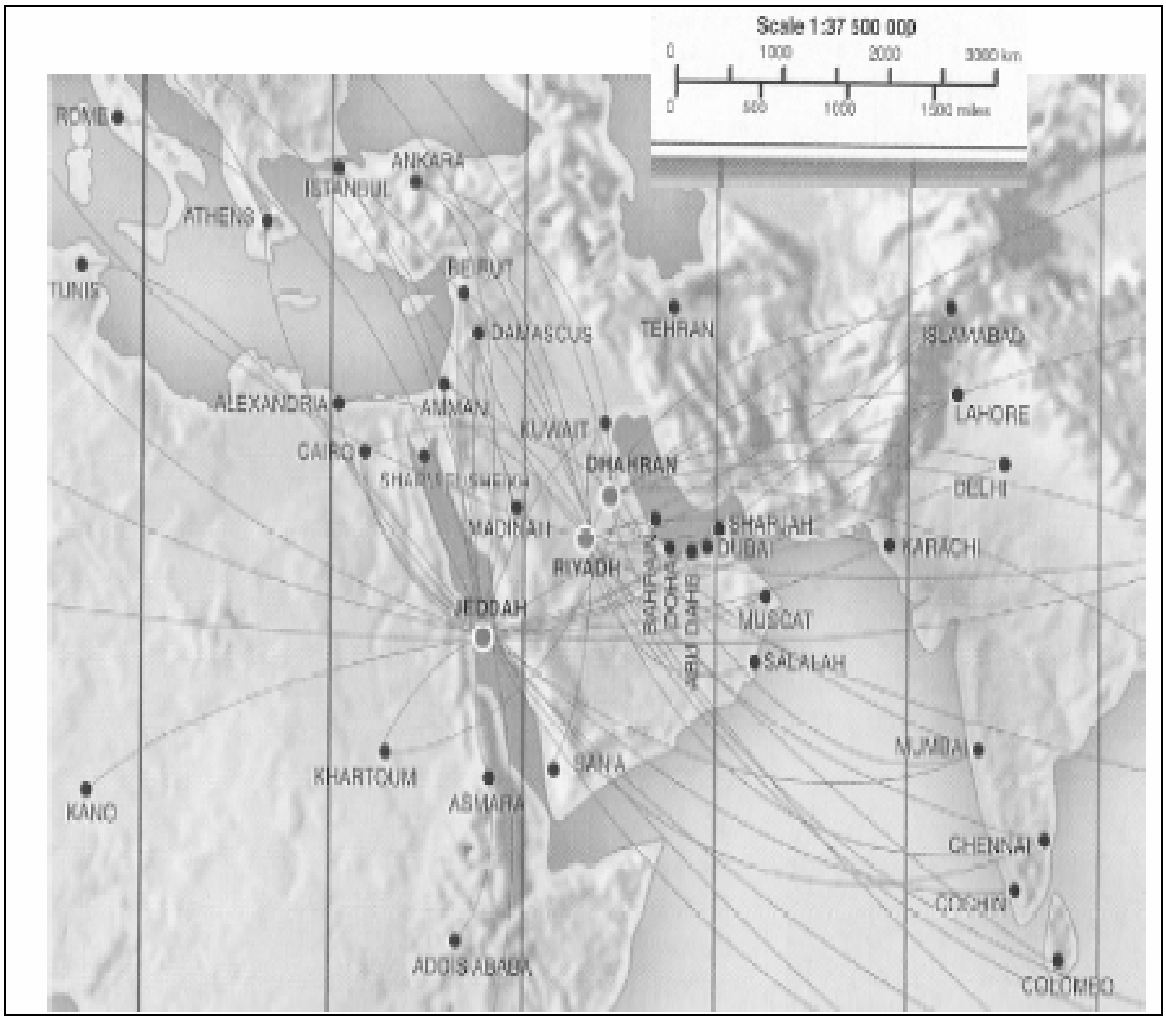

Figure 2.6 Regional routes in Saudi Arabia & Gulf Region

1.2.7 Regional Aircraft in Service with SA Airlines and their Cost

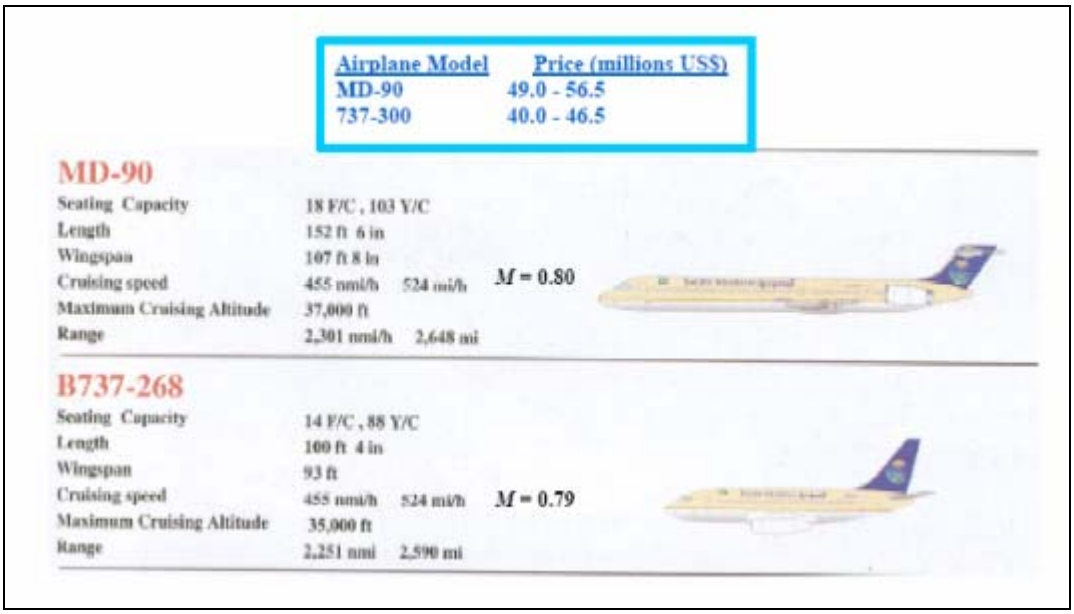

Figure 2.7 Regional Aircraft in Service with SA Airlines and their Cost

2. Problem Statement

2.1 Synopsis

The ever-increasing dependence and demands for fossil fuels coupled with a limited supply of such fuels in near future suggests a need to investigate the feasibility of designing a 80-100 seat commuter aircraft incorporating advanced technology in airframe and engine designs that is not only fuel efficient but economical (less than US $ 60 million) to operate with minimum serviceability and support.

2.2 Project Objective

The objective of this year's project is to design an 80-100 seat commuter aircraft capable of transporting passengers and baggage along principal air routes within the Kingdom and the Gulf region. Consideration should be given to minimizing direct operating costs and cost per passenger miles in terms of fuel consumption, simplifying maintenance operations while incorporating advanced technology in airframe and engine designs.

2.3 Project Requirements:

According to the survey, we need to design a regional aircraft that has the following characteristics:

- Mission Profile
  - – Warm Up/Taxi for 10 min, sea level, standard day.
  - – Take off within distance specified in Special
  - – Climb at best rate of climb to cruising altitude of 36,000 ft.
  - – Cruise at *V* best range (knots) for best range (nm).
  - – Land with reserve fuel for additional 100 nm range and 45 min loiter at 5000 ft.
  - – Taxi to gate for 10 min, sea level, standard day 30 c^{o}.

- Special Design Requirements
  - – Takeoff Distance (FAR 25 Balanced field length)
    - • Concrete: sea level standard day < 5000 ft. at max TOGW
  - – Climb Performance:
    - • Two engine sea level standard day climb rate > 2100 fpm
  - – Cruise Performance:
    - • Best range velocity V of 0.8 Mach number for best range of 1500 nm or more and grater than 300 kts true airspeed at 36,000 ft.

– Cabin Size:

- 80-100 passengers (200 lb/ person includes baggage)
- 2 crew, 3 flight attendants (200 lb/ person)
- 2 lavatories
- Seat pitch at least 31 in.
- Baggage volume > 11 cubic feet per pax (880-1100 cubic ft., includes under seat, overhead, closets and main baggage compartment)
- Aisle height > 72 in

2.3 Mission Profile:

The aircraft will be mainly designed according to the following mission profile:

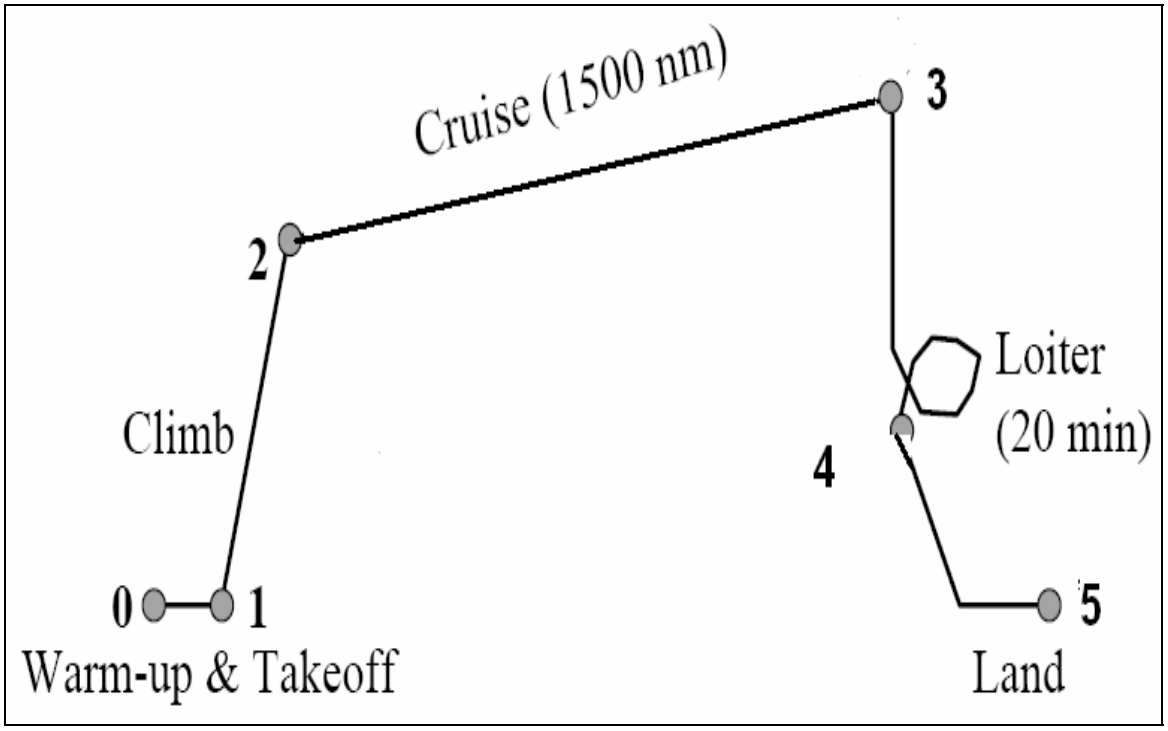

Figure 2.7 Aircraft mission profile

2.4 Approach:

Actually in this design project we follow exactly step by step the aircraft design techniques in Raymer's book (aircraft design: A conceptual Approach).
The class is divided into different seven groups. Each student is assigned a major task and a minor task as the following table shows:

Table 3.1 Design project groups tasks

Category	Major	Minor
Project leadership	Salman AL-Fifi	Ghassan Gawwas
Aerodynamics	Uthman Mushari	Ali Abatahin
Propulsion systems	Abdullah Barrak	Ghassan Gawwas
Performance & stability	Khaled AL-Anazi	Salman AL-Fifi
Weight & balance & Structures	Mohammed Nwaser	Abdullah Barrak
Advance technology	Mohammed Nwaser	Ali Abatahin
Computer Graphics	Ghassan Gawwas	Uthman Mushari
Market survey & cost analysis	Ali Abatahin	

Then timetable for the project from the beginning of the semester till the end of the semester is as follows:

Table 3.2 Timetable of design process

Week 2	Distribute missions
Week 3	Looking to aircraft data + mission profile
Week 4	engine data (3 turbofan)
Week 5	weight estimation + (T/W), (1^{st} stage)
Week 6	aircraft rough sketches
Week 7	Aircraft dimensions
Week 8	weight estimation + (T/W), (2^{nd} stage)
Week 9	Different Systems locations
Week 10	Preliminary layout configuration
Week 10-15	Readjust layout + redo all analysis and cost studies + writing the final report

3. Initial Sizing and Layout

3.1 Introduction

Before the structure can be designed, we need to determine the loads that will be imposed on the aircraft. This section deals with the general issue of aircraft loads and how they are predicted at the early stage of design process.

Each part of the aircraft is subject to many different loads. In the final design of an aircraft structure, one might examine tens of thousands of loading conditions of which several hundred may be critical for some part of the airplane. In addition to the obvious loads such as wing bending moments due to aerodynamic lift, many other loads must be considered. These include items such as inertia relief, the weight and inertial forces that tend to reduce wing bending moments, landing loads and taxi-bump loads, pressurization cycles on the fuselage, local high pressures on floors due to high-heeled shoes, and many others.

These loads are predicted using Navier-Stokes computations, wind tunnel tests, and other simulations. Static and dynamic load tests on structural components are carried out to assure that the predicted strength can be achieved. The definition of strength requirements for commercial aircraft is specified in FAR Part 25 and this section deals with those requirements in more detail.

3.2 Initial Sizing

- First of all we started to estimate the initial gross weight by finding the weight of each mission segments. The results of these calculations are listed below.

Table 3.1 mission segment weight fractions

Engine start, taxi and takeoff	
W1/W0	0.98
Climb and accelerate to cruise altitude and M	
W2/W1	0.9797525
Cruise	
W3/W2	0.861327303
Descent to 5000 ft	
W4/W3	0.995
Loiter	
W5/W4	0.98167922
Descent to SL	
W6/W5	1
Reserve Range	
W7/W6	0.985170447
Landing and taxi back	
W8/W7	0.995
Mission weight fraction	
W8/W0	0.791840672

- The after we do some iteration we found that our total design gross weight would be ***86011 lbm.***

- In addition we found the thrust to weight ratio for some mission segment. Results are found to be as follows.

Table 3.2 T/W Values

Description	**T/W**
Statistical estimation	0.25
T/W_o	0.2496
$T/W_{takeoff}$	0.18267
T/W_{cruise}	0.0996

- Then, we calculated the wing loading and we got the following results.

Table 3.3 Wing loading Summary

Mission leg	**at W,leg (lb/ft^2)**	**W/S at W, TO**	**Area Calculated (ft^2)**
W/S_stall	75.20	75.20	407.3688197
W/S_takeoff	77.10	77.10	397.2900303
W/S_takeoff climb	98.32	98.32	311.5543471
W/S_landing	64.81	77.47	395.3947336
W/S_cruise	124.96	130.79	234.2139116
W/S_loiter	50.81	58.88	520.2501284

- There are several critical aspects that play a major role in the selection of Thrust-To-Weight and wing loading. Those are:
    a. The lowest value of W/S should be selected to ensure that the wing is large enough for al flight conditions. In this step we should convert all wing loadings to takeoff conditions prior the comparison.
    b. When the best w/s has been chosen, the thrust-to-weight ratio should be recalculated.

- The previous steps are summarized in the following tables.

Table 3.4 T/W check at takeoff

Assume T/W	G (Eq. 5.31)	W/S (Eq. 5.30)
0.15	0.067	29.63
0.25	0.167	29.63
0.2	0.117	29.63
0.225	0.142	29.63

- In the above table we chose 0.25 because it derives the takeoff C_L (in Eq. 5.9 and Fig. 5.4 in the book)

Table 3.5 W/S Check

Assume S (ft^2)	**Mission Leg**	**W,leg (lb)**	**W/S,leg psf**	**Mission spec**	**Required**	
968.75	W/S_stall	67544.75	69.72	CL,max	2.41	**Keeping in mind Fig. 5.3**
968.75	W/S_takeoff	67544.75	69.72	CL,TO	2.32	
968.75	W/S_landing	56500.28	58.32	CL,max	2.34	**Keeping in mind Fig. 5.3**
968.75	W/S_cruise (AR=2.44)	64535.63	66.62	b, ft	48.6	
968.75	W/S_loiter (AR=12.03)	58291.73	60.17	b, ft	107.97	

- So, we'll get the following results.

Table 3.6 Select Choices

S (ft^2)	**968.75**
AR	**8.6**
B (ft)	**91.28**
TOGW (lb)	**67544.62**
W/S_TO	**69.72**
T/W	**0.23**
CL,max	**3.20**
CL,TO	**3.10**

In table 3.6, we choose the specified area because it gives a reasonable C_{Lmax}. And T/W because it gives climb gradient G>0 and reasonable $C_L$at takeoff. Regarding C_{Lmax}, we should keep in mind figure 5.3 in the textbook.

3.3 Initial Layout

3.3.1 The cross-section of the aircraft

For our design aircraft which can carry 100 passengers, the following requirements for the cross section are shown in table (3.7)

Table 3.7 Aircraft Cross Section

Seat pitch	0.9144	m
Seat width	0.4572	m
Headroom	1.6002	m
Seat layout	3-0-2	
Number of seats	100	
No. of seat rows	20	

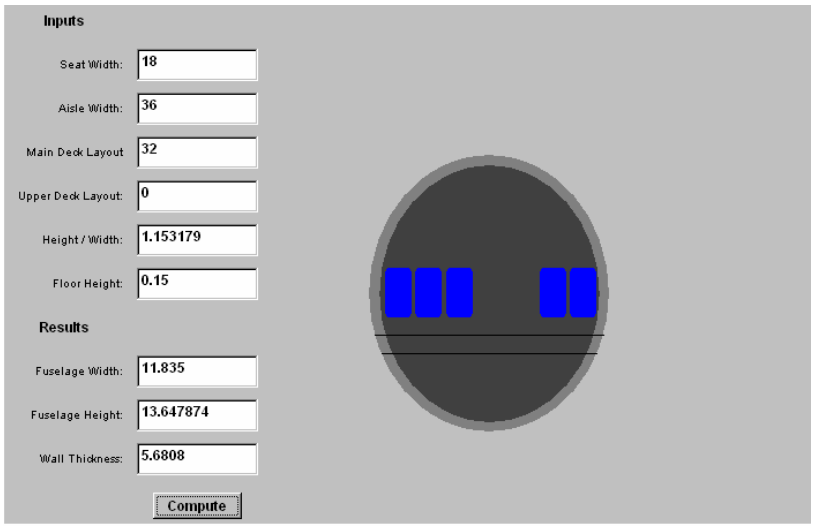

Figure 3.1 Aircraft Cross Section by using the Java applet

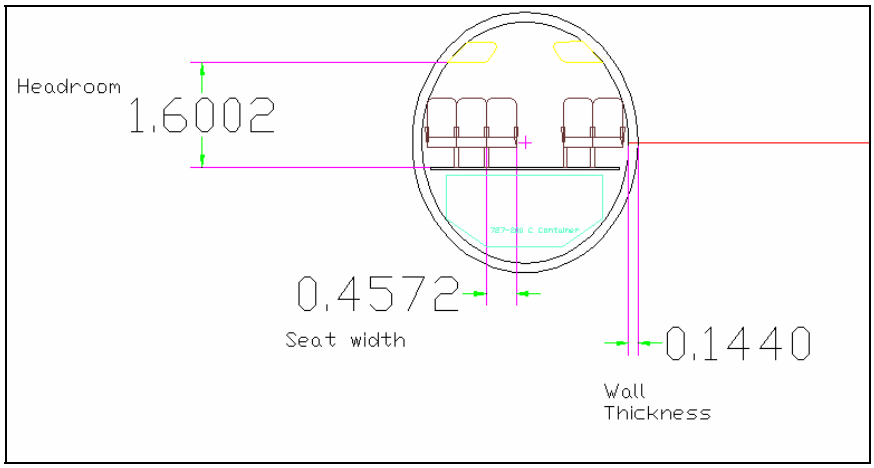

Figure 3.2 Aircraft Cross Section by using AutoCAD

3.3.2 The top view of the aircraft:

Table 3.7 Fuselage dimensions

DIMENSIONS	
Fuselage:	
Length (m)	29.79
Height (m)	3.99
Width (m)	3.46
Finess Ratio	8.84

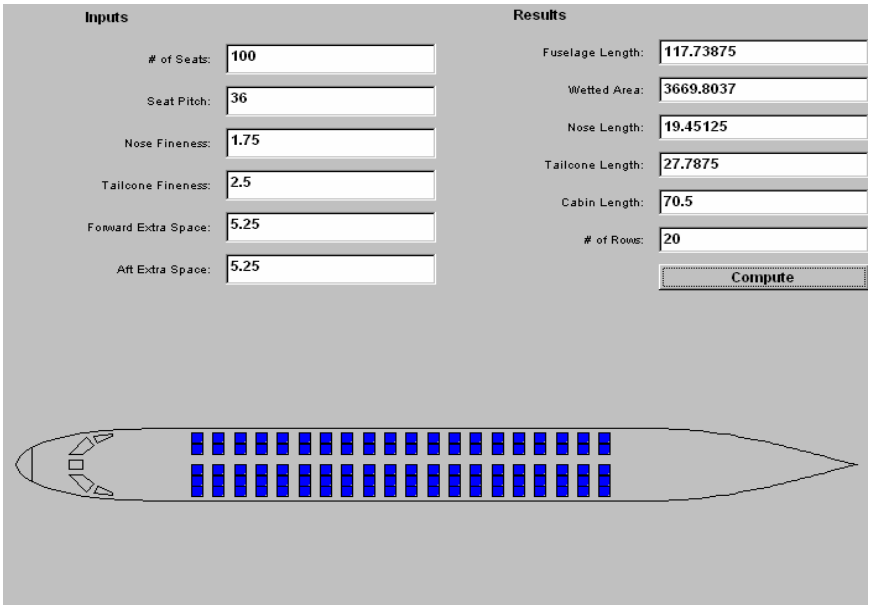

Figure 3.3 The top view of the aircraft by using the Java applet

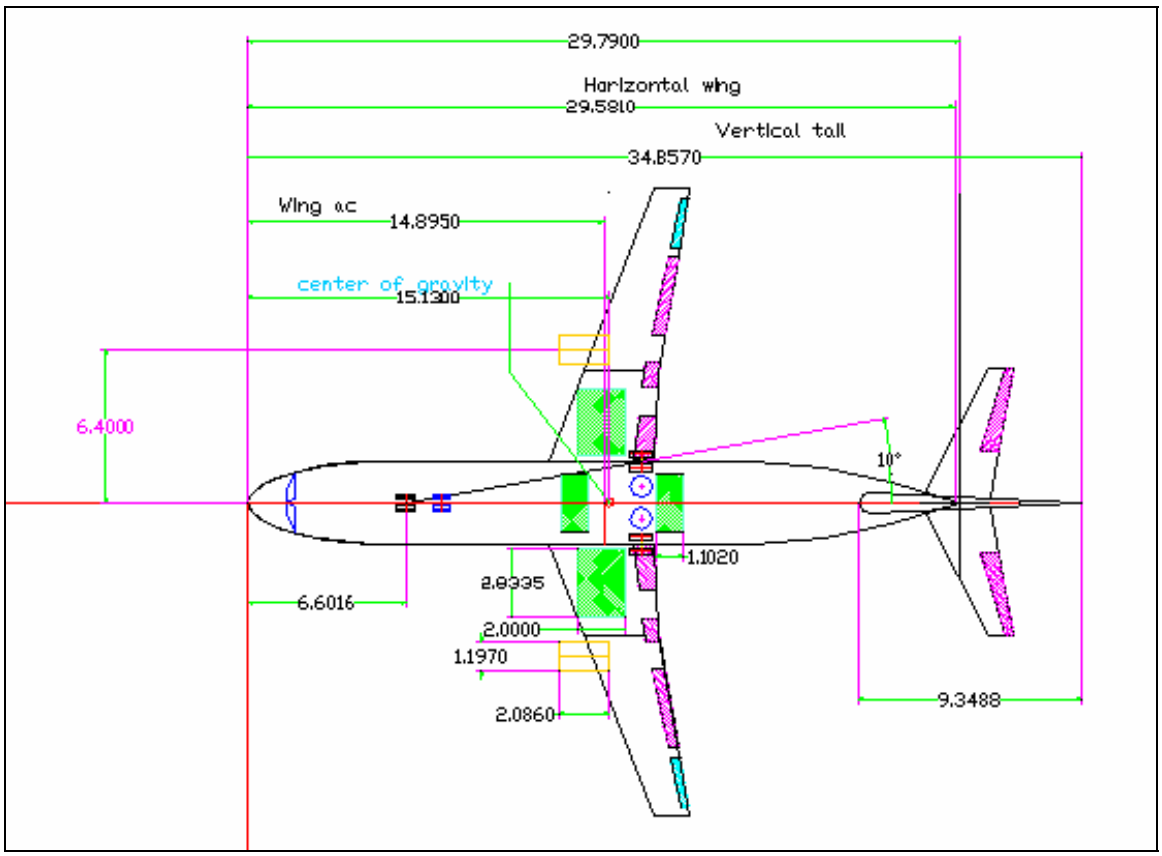

Figure 3.4 The top view of the aircraft by using AutoCAD

3.3.3 The Side View:

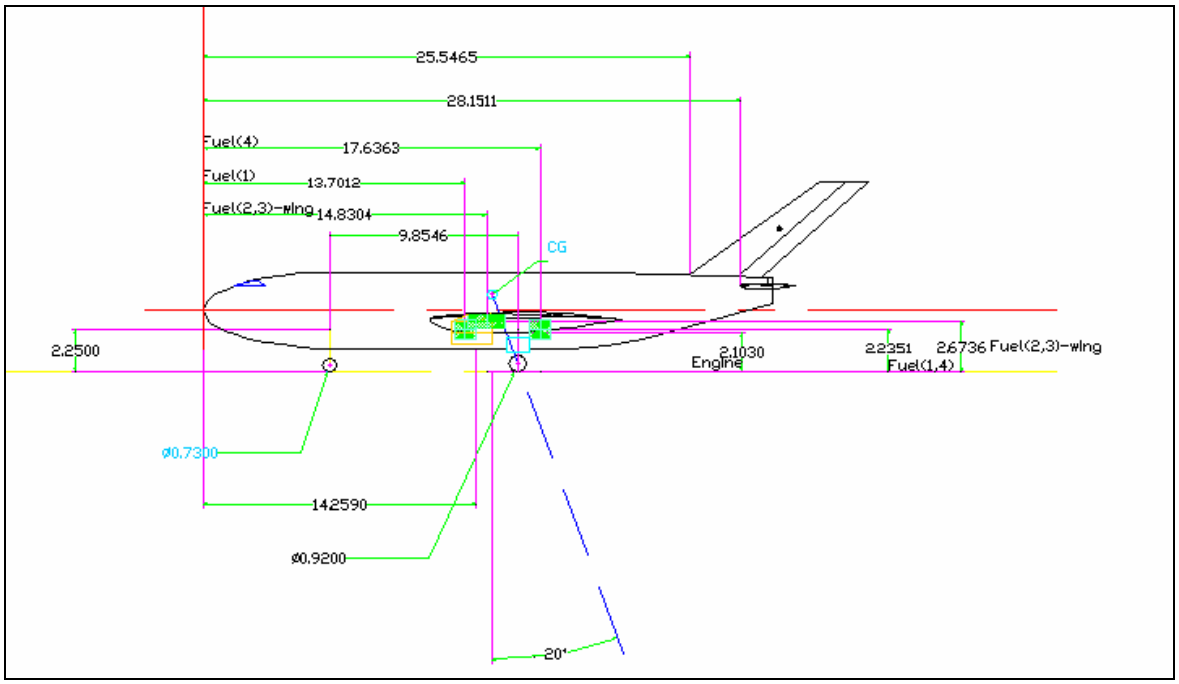

Figure 3.5 The Side View of the Initial Layout

3.3.4 The Front View:

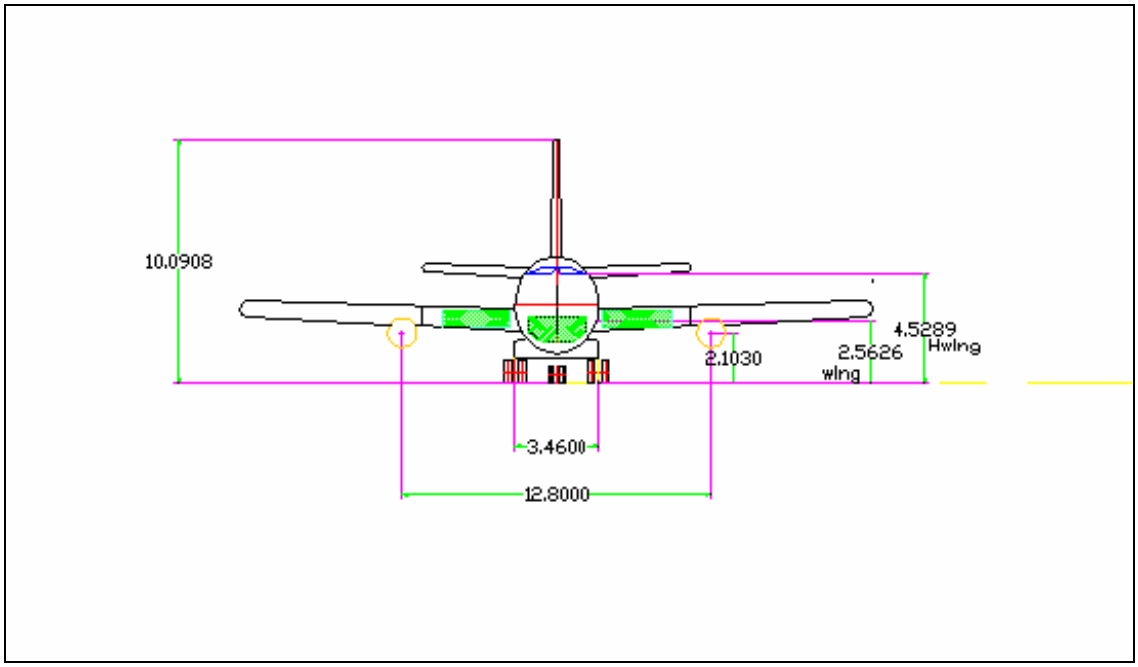

Figure 3.6 The Front View of the Initial Layout

3.3.5 The cross-sectional view with the front view:

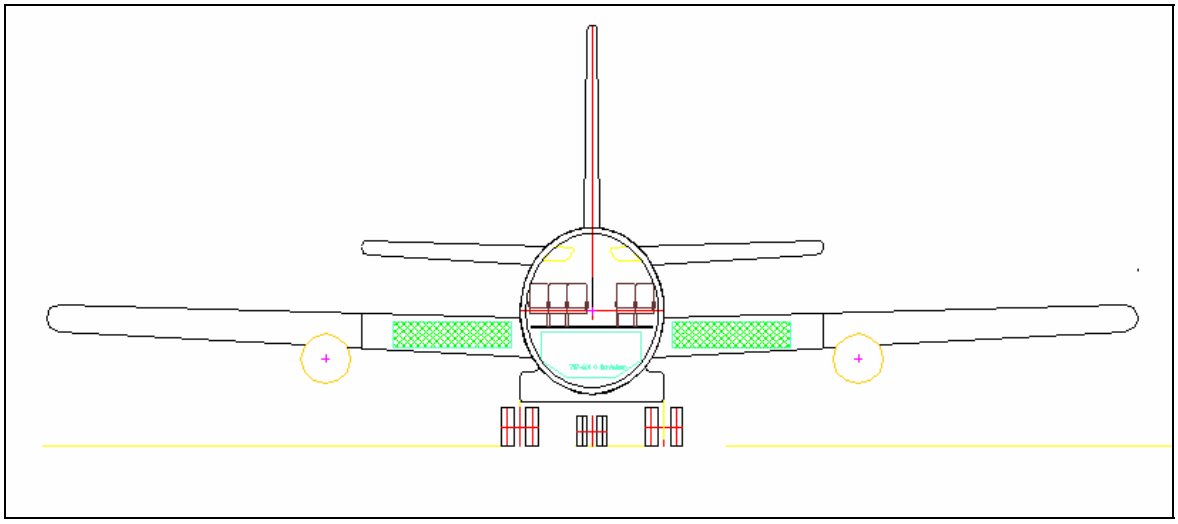

Figure 3.7 The cross-sectional view

As seen from figure (3.6): the wing, horizontal tail and the vertical tail are very thick. But in the final layout, these problems are fixed.

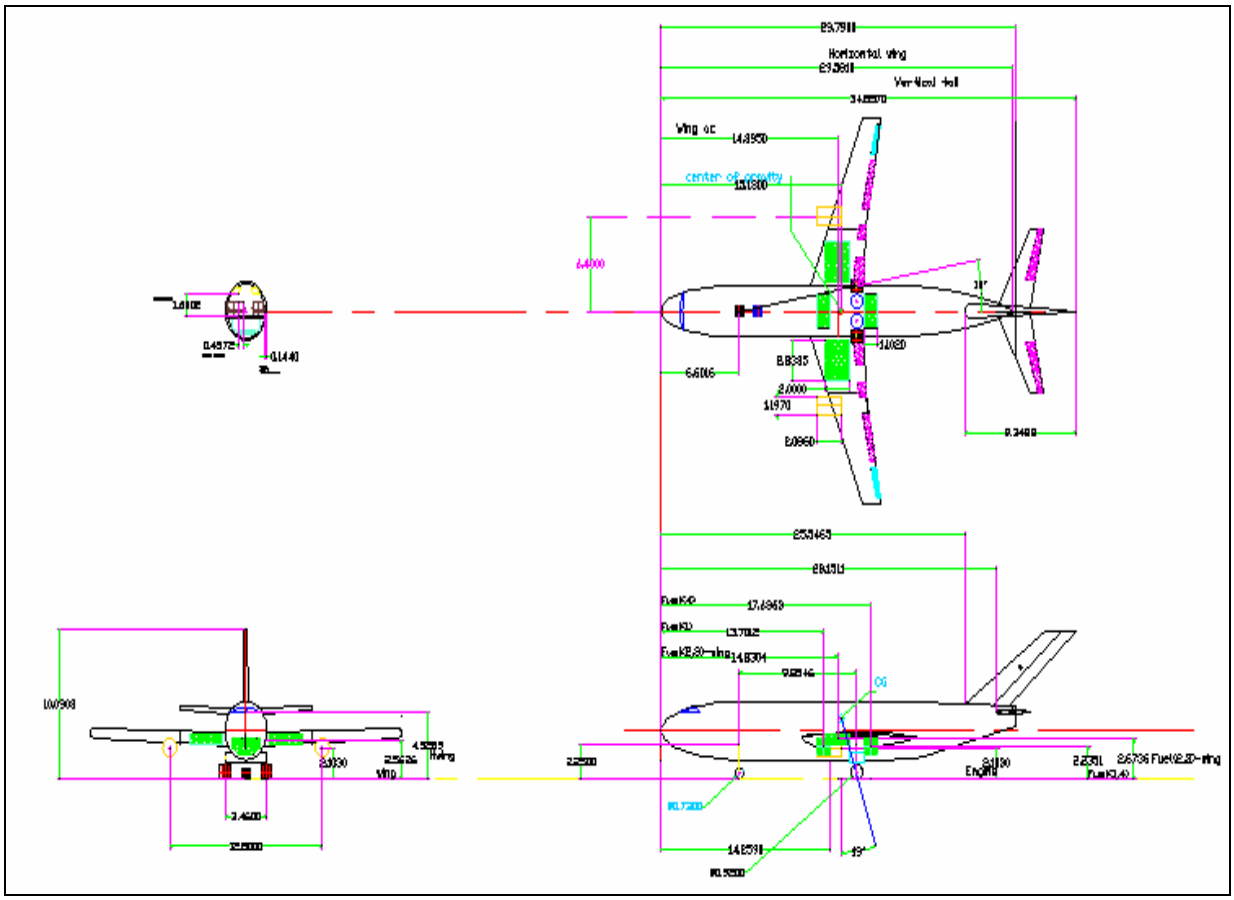

Figure 3.8 The 3 view of the Initial Layout

4. Propulsion and Fuel System

4.1 Specifications and Requirements based on initial sizing:

From the initial sizing, the thrust/ weight required is 0.25 which suggest a required thrust at takeoff =21502.75 lb.
In this project, we will consider a rubber engine design scaled to achieve the requirements. For this we choose (High Bypass Turbofan Engine) HBTF engine data from reference (Appendix B.4-2) that has been scaled to meet the current design needs. Thus, the scale factor for the rubber engine is:

$$SF = \frac{T_{required}}{T_{actual}} = \frac{49350(kN)}{50{,}000(\ fromA - 4.2)} = \frac{11{,}094lb}{50{,}000lb} = 0.2219$$

The dimensions for the scaled engine are then:

$$L = L_{actual}(SF)^{0.4} = (150)(0.2219)^{0.4} = 82.14in = 2.086m$$
$$D = D_{actual}(SF)^{0.5} = (100)(0.2219)^{0.5} = 47.11in = 1.197m$$
$$W = W_{actual}(SF)^{1.1} = (7700"\ fromA - 4.2")(0.2219)^{1.1} = 1469.82lb$$

4.2 Engine performance Curves

The following installed-engine data reflects these assumptions:

1) Inlet total pressure ratio of 0.97.
2) Power extraction of 650 kW to drive electric generator and auxiliary equipment at all power settings and flight conditions.
3) High-pressure bleed airflow at rate of 2.0 lb/s.

4.3 Fuel System:

Table 4.1 Fuel System

Fuel volume (Table 10.5)		
Total fuel volume	10.902	cu.m
Fuel volume in wings	7.25	cu.m
Fuel volume aft of cg	2.21	cu.m
Fuel volume fore of cg	2.21	cu.m

All the fuel tanks placements and locations are shown on the AutoCAD layouts.

4.3.1 Fuel Volume Distribution:

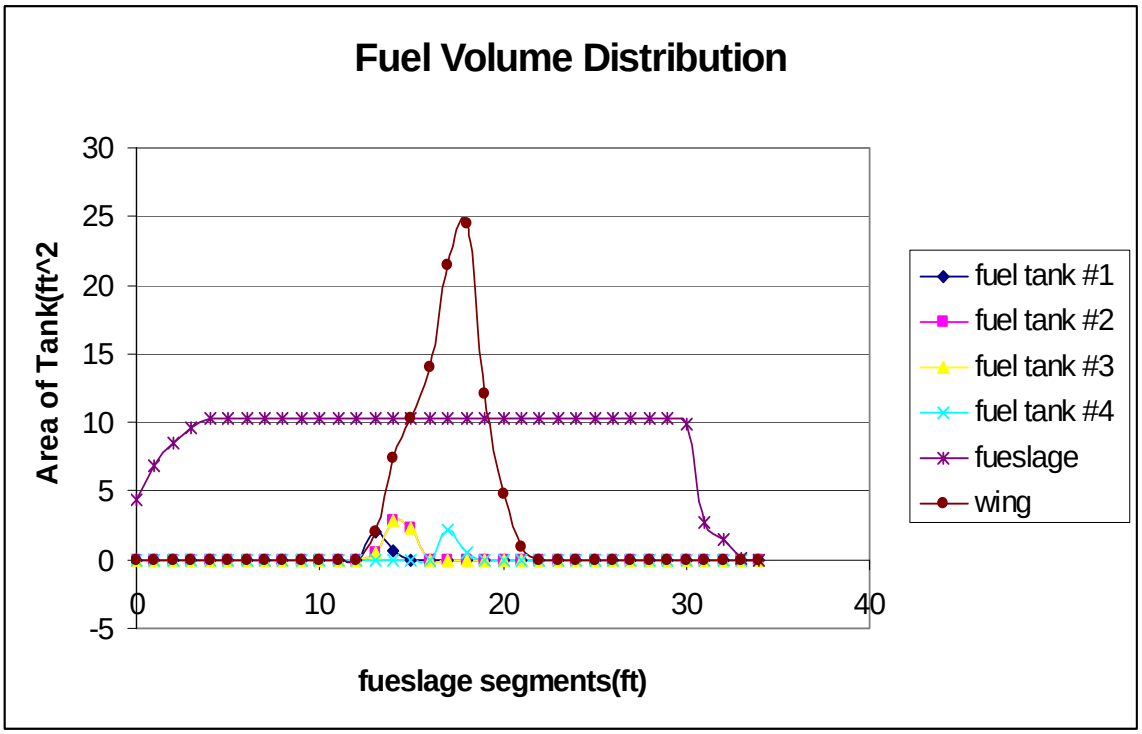

Figure 4.1 Fuel volume distribution

5. Aerodynamics

In aerodynamics part of our design project we will follow the following steps: first, we will design the wing and tails airfoils. Then, we will specify our aircraft dimensions based on the mission request. After that, wing and tail geometries will be chosen. Finally, we will calculate the aerodynamic coefficient forces.

5.1 Airfoil design

There will be two different kinds of airfoils, which will be used. The first one will be used for the wing, while the other will be for both of horizontal and vertical tails.
Because of that, the wing is considered as the main part of the aircraft and it is facing the most forces that produced from aerodynamics flow. There for, we will need to design a modern airfoil for the wing. Then, we will use a java program that is in Sanford website (Ref. 5). The type of wing airfoil is NACA 64A010; which is shown in figure 5.1.

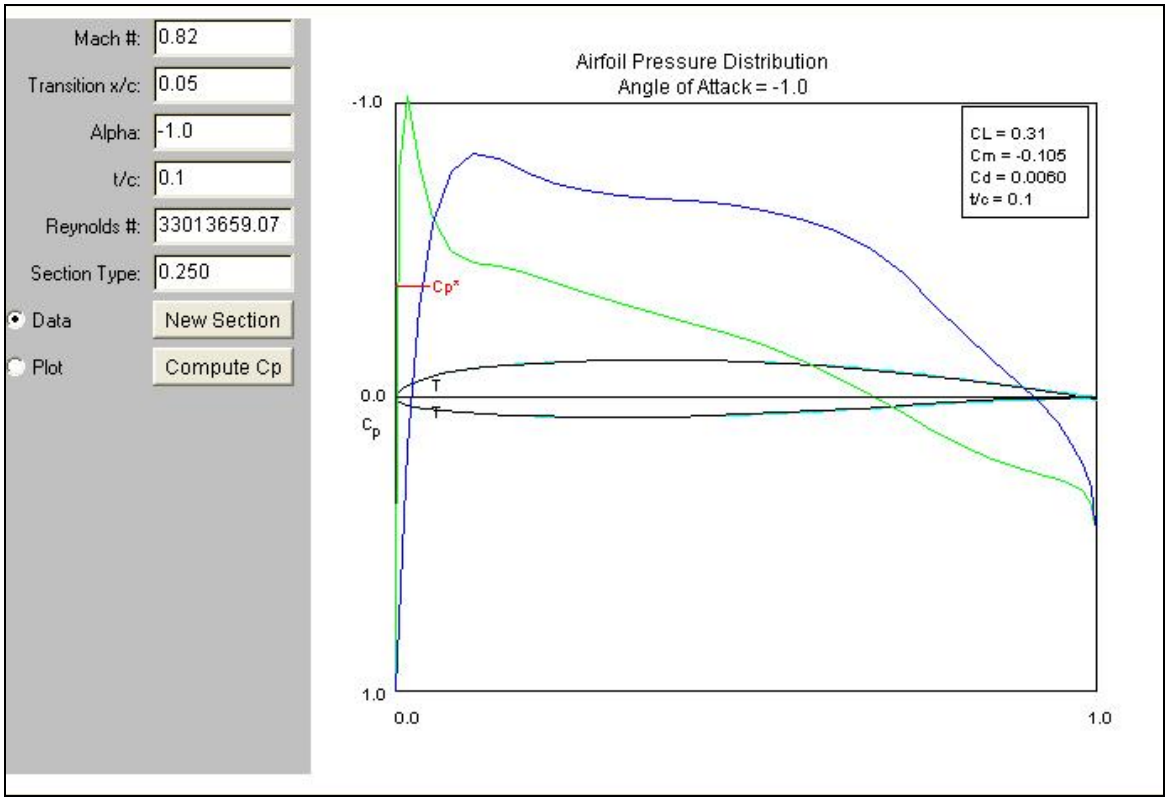

Figure 5.1 Wing Airfoil
The program used for wing airfoil designing from Ref. 5

On the other hand, for the horizontal and vertical tails we will use a symmetric airfoil, which will be same for both. This airfoil kind will be NACA 0010. To design this airfoil, a java program including in Pagendarm website (Ref.8) will be used. The airfoil is shown in figure 5.2.

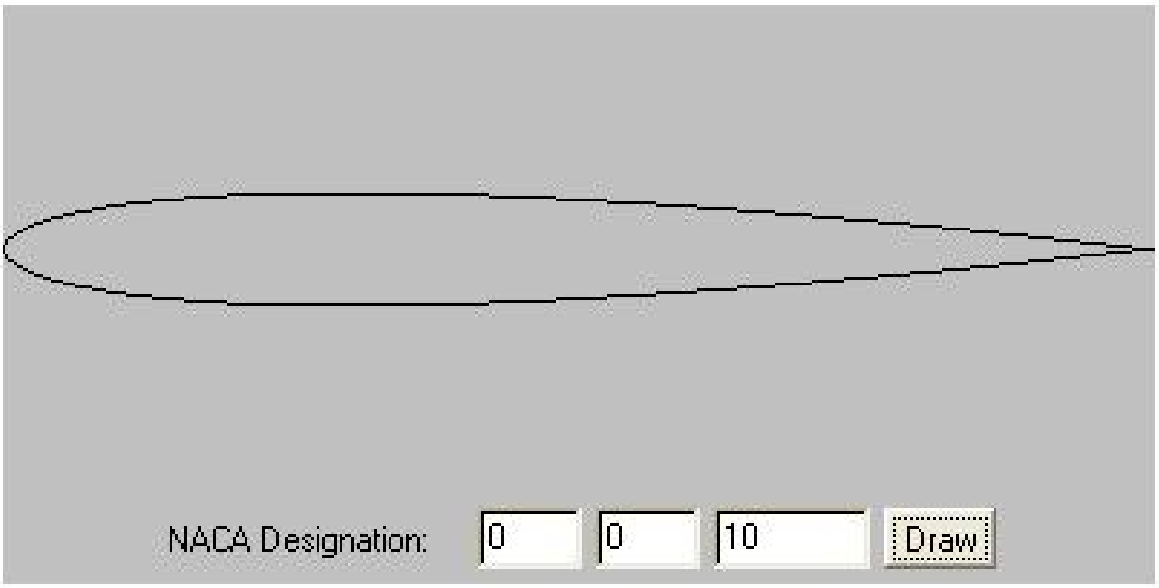

Figure 5.2 Tail Airfoil (Shape) Sample of the tails airfoil shape

5.2 Aircraft dimensions

Our aircraft dimensions are based on mission required. Also some historical data will be used here. These dimensions are included in appendix D.1.

5.3 Wing and tail geometry

Basing on dimensions chosen and the missions required the wing geometry would be designed. From the same java program included in Stanford website (Ref. 5) will be used for design the wing geometry, see figure 4.3. Also figure 4.4 shows tail geometry.

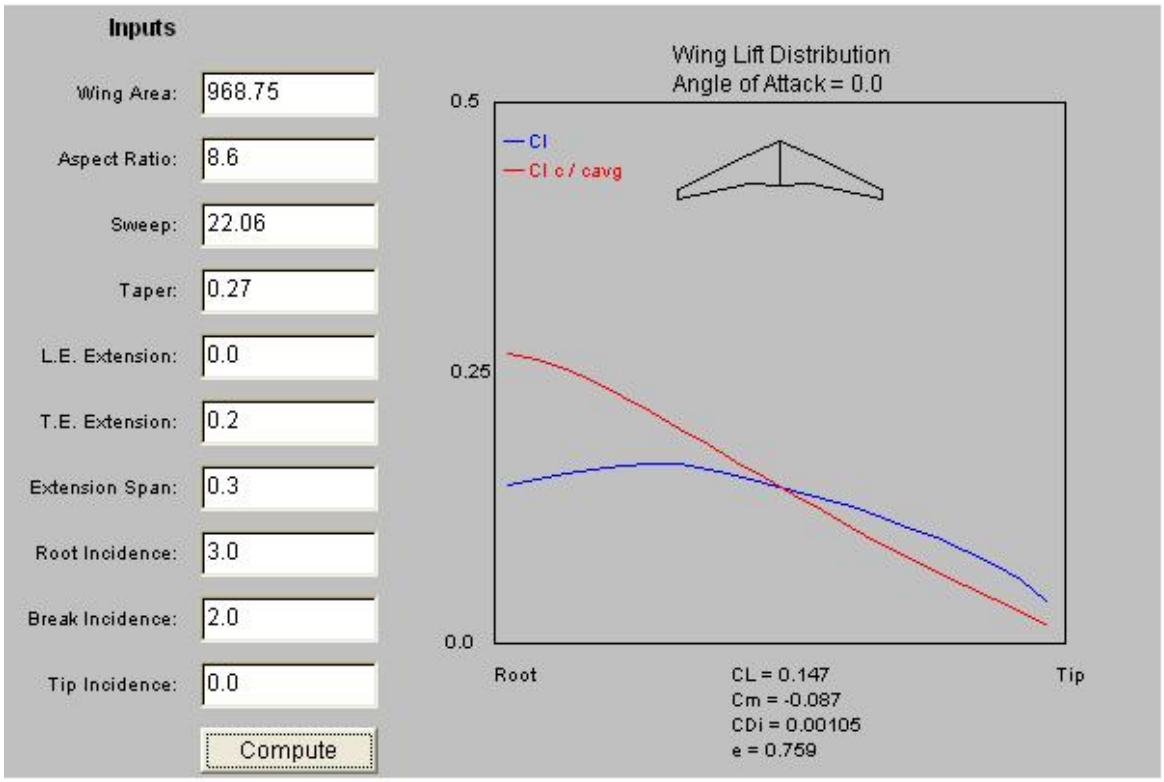

Figure 5.3 Wing Geometry
Java Stanford program (Ref. 5) used to design the wing geometry

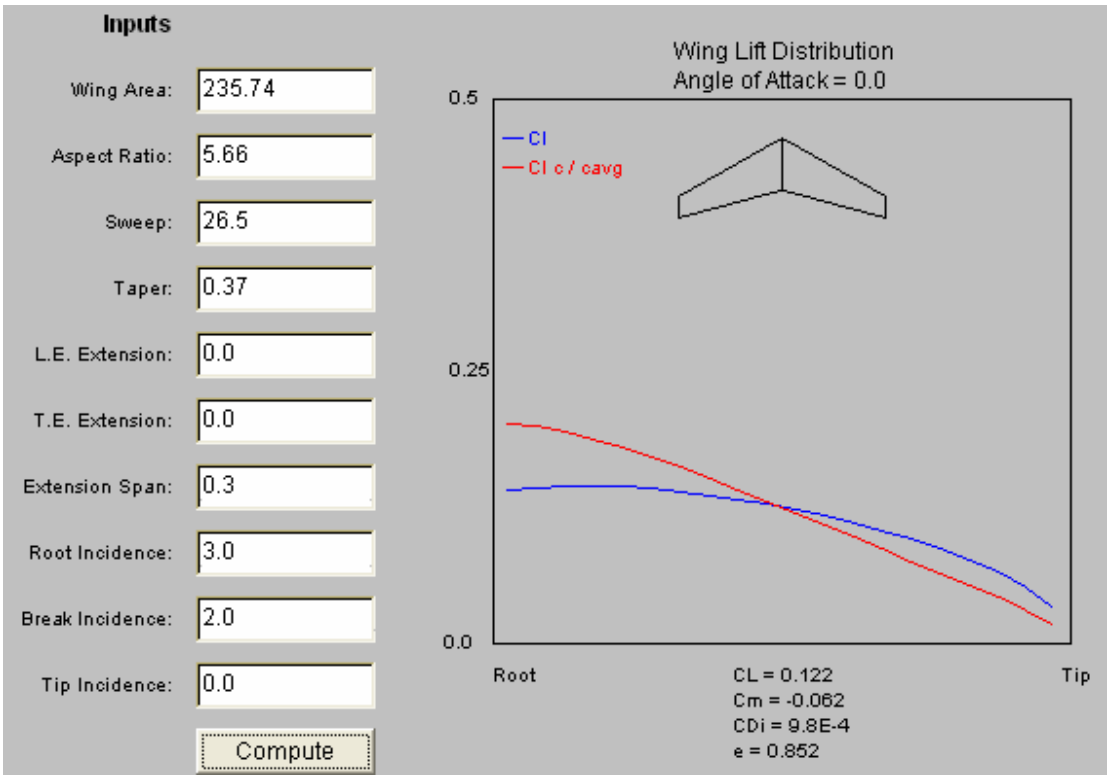

Figure 5.4 Tail Geometry
Java Stanford program (Ref. 5) used to design the Tail geometry

5.4 Force coefficients

There are two main forces affect on the aircraft, which are lift and drag forces. Usually these forces are specified by there coefficients, which are dimensionless.
In this part we will at the beginning calculate constant variables that will be needed for calculating the forces coefficients. After that, we will calculate the lift force coefficient for the wing and horizontal tail, and also examine the relation between lift coefficient and angle off attack. Also, we will test the effect of flap hinge angle on maximum lift coefficient. After that we will calculate the drag coefficient and see the relation between lift and drag coefficients.

5.4.1 Useful variables

A mat lab programs shown in appendix D.2, is used to calculate the following variable data: Reynolds number, Re, Oswald span efficiency factor, e, and K.
These variables are needed for calculating the forces coefficients. For cruise stage, h = 30000 ft, we found that:
Re = 27521000
e (for wing) = 1.3782 e (for tail) = 1.4129
K (for wing) = 0.0269 K (for tail) = 0.0398

5.4.2 Lift coefficients (C_L)

First, we will calculate C_L for wing. The same Stanford java program (Ref. 5) will be used in order to study the effect of angle of attack (Alpha) on C_L at 2 dimensions, airfoil. The above figure 5.1 shows the sample of program that read different values for C_L with different angle of attack. After collecting data from that program, see data at appendix D.3.Then, $C_{L\alpha}$ ($=\partial C_L / \partial \alpha$) and maximum C_L can be calculated from following figure, figure 5.5.

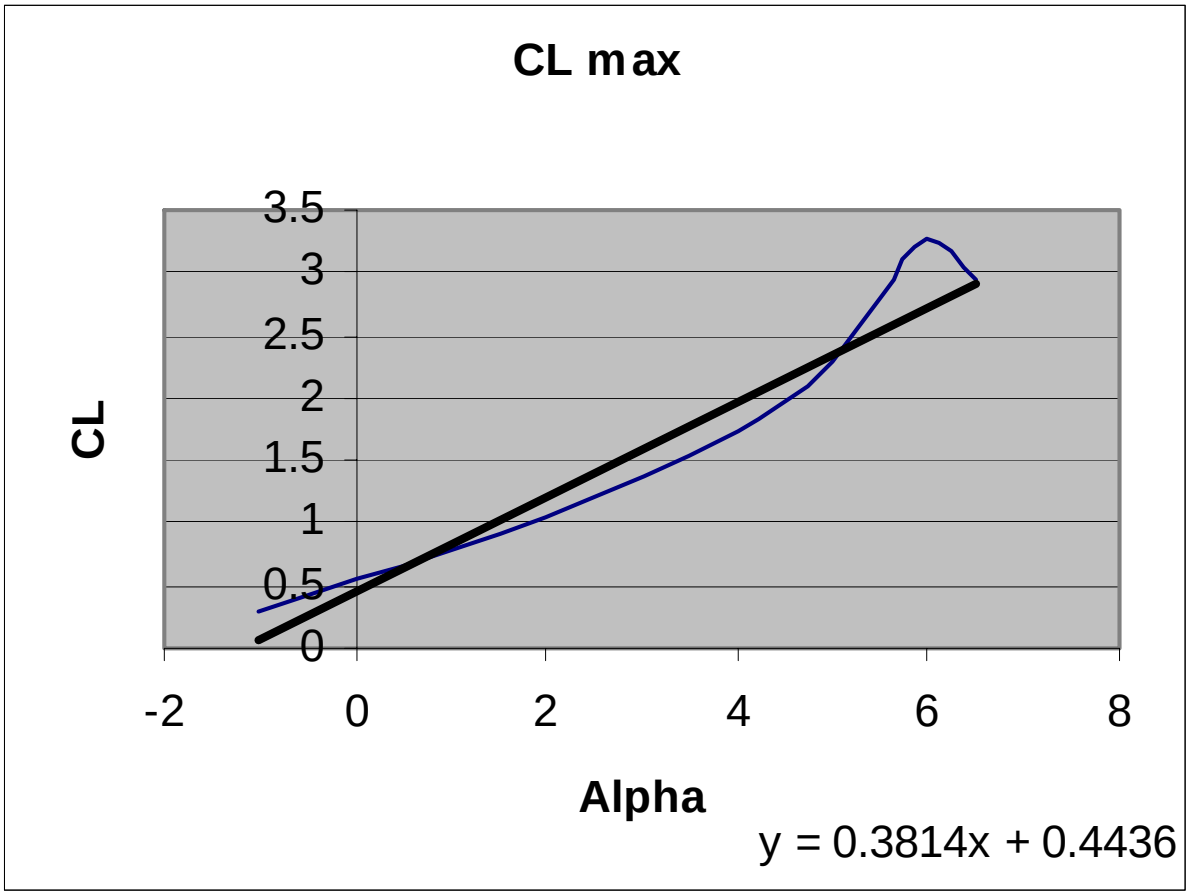

Figure 5.5 C_L vs. Alpha (W)
Showing $C_{L\max}$ and $C_{L\alpha}$ (The slop)

There for, $C_{L\alpha} = 0.3814$

And $C_{L\max} = 3.28$

While for 3-Dimension wing a Mat lab program is used, see appendix D.4, to calculate $C_{L\alpha}$ and $C_{L\max}$, for 3-D.

$C_{L\alpha} = 0.1221$/deg

$C_{L\max} = 2.7303$

Second step, C_L with 2 dimensions for horizontal tail will be calculated. Using Pablo program at Matlab (Ref. 7) in order to calculate the relation between C_L and angle of attack (alpha). Figure 5.6 shows this program.

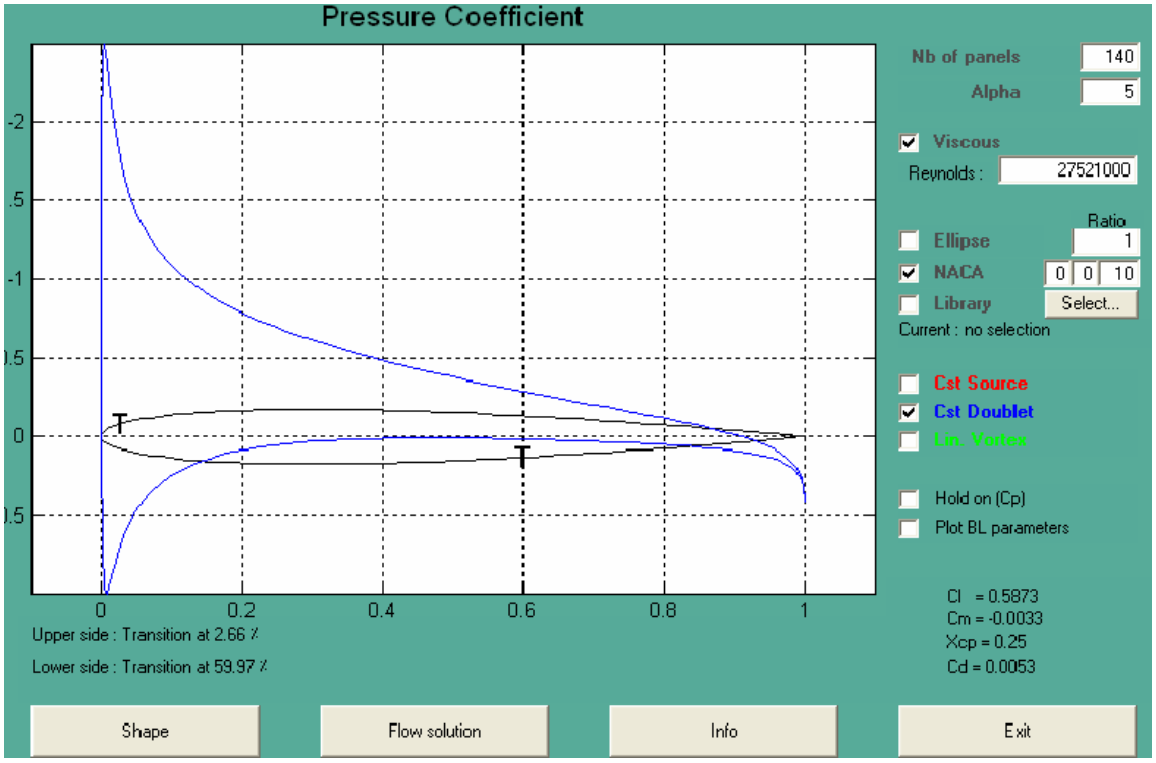

Figure 5.6 Pablo Program
Sample shows the program used for calculating CL vs. alpha in h-tail

After collecting data in Excel sheet included in appendix D.5, then figure 5.7 was plotted in order to find $C_{L\alpha}$ and C_L max in 2-dimensions for h-tail airfoil.

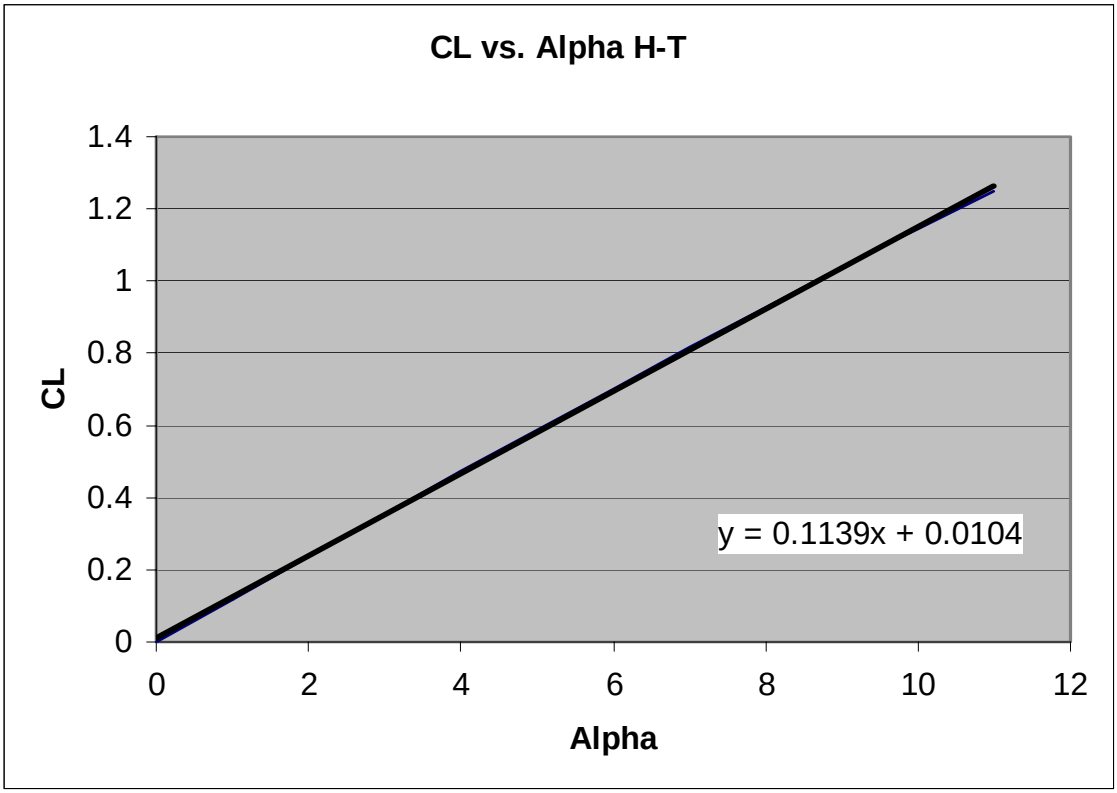

Figure 5.7 C_L vs. Alpha (H-T)
Calculating $C_{L\max}$ and $C_{L\alpha}$ at 2-D for h-tail

There for, $C_{L\alpha} = 0.1139$
And $C_{L\max} = 1.1436$
(Note: at alpha = 10 deg, we assumed $C_L = C_{L\max}$ because after 10 deg separation increase and its effects appear with C_D, see figure 5.8).

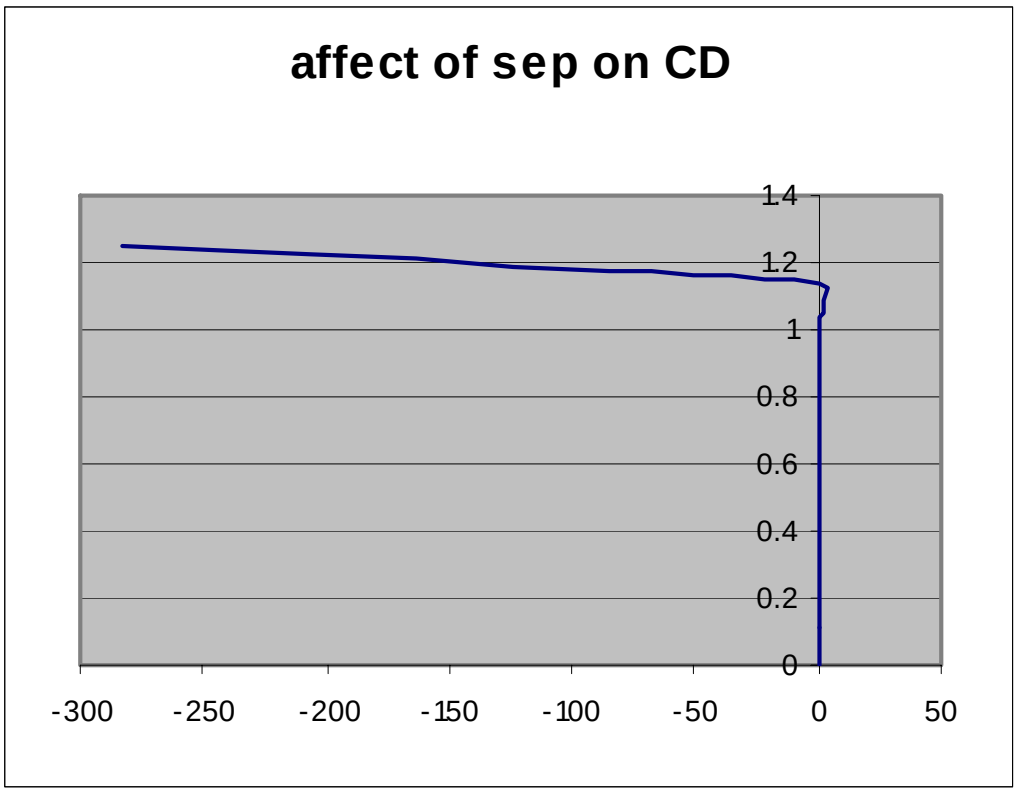

Figure 5.8 CD vs. Alpha
Affect of high alpha on CD for h-tail because of separation

At the same previous way, C_L's for 3-D h-tail were calculated using Matlab program in appendix D.6. We gut that:
$C_{L\alpha}$ = 0.1416/deg
$C_{L\max}$ = 0.9223

5.4.3 Drag coefficient (C_D)

Different values for CD in both wing and h-tail airfoils were calculated at the same way for CL and the data will be including in appendix D.3&5.
For the 3 dimension wing and tail:
C_D (wing) = 0.1306
C_D (tail) = 0.0324
Where a Matlab program was used for this calculating is including in appendix D.7.

5.4.4 Flap effect

Flap is a horizontal control surface founding in the wing. It used basically to increase the $C_{L\max}$. We used the Stanford java program (Ref. 5), which is shown figure 5.9, to observe it affects on both C_L and C_D. In appendix D.8, the data collected from the program for C_L and C_D in 3-dimensions with different flap hinge angles (F.H.A) is there.

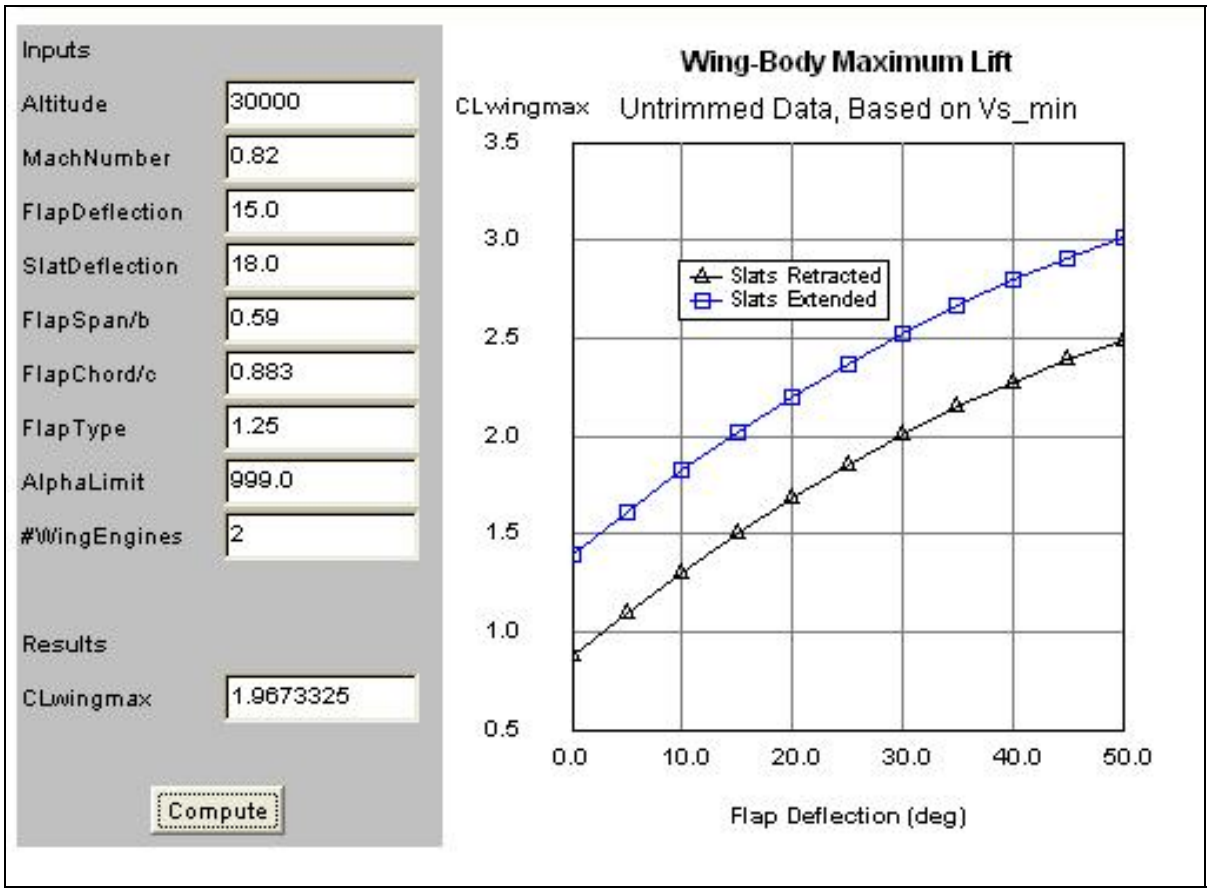

Figure 5.9 C_L change with Flap
Stanford program used to calculate CL & CD for different F.H.A.

In figure 5.10, we can note that $C_{L\max}$ is increasing slightly with the increasing of hinge angle of the flap, while C_D is also increasing, but sharply, with increasing of the hinge angles, see figure 5.11.

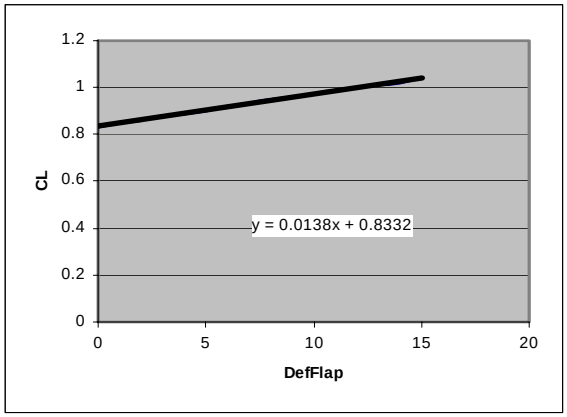

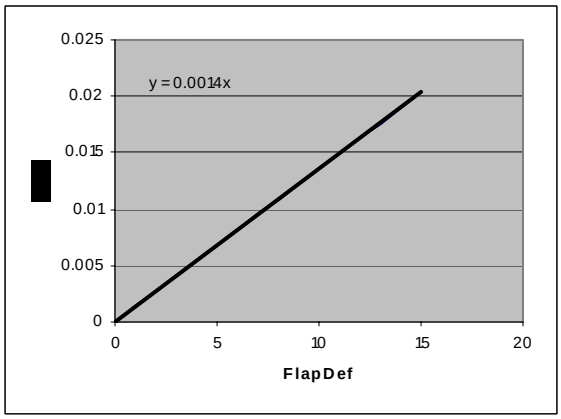

Figure 5.10 C_L vs. F.H.A

Figure 5.11 C_D vs. F.H.A

$C_{L\max}$ increasing slightly while C_D is sharply with different F.H.A

From these two figures we can conclude that flap is using to increase drag besides increasing lift and that to help aircraft during landing (as additional breaks).

4.4.5 C_L / C_D

In appendixes D.3, 5&8, we used the data, which is there to plot the following figures.

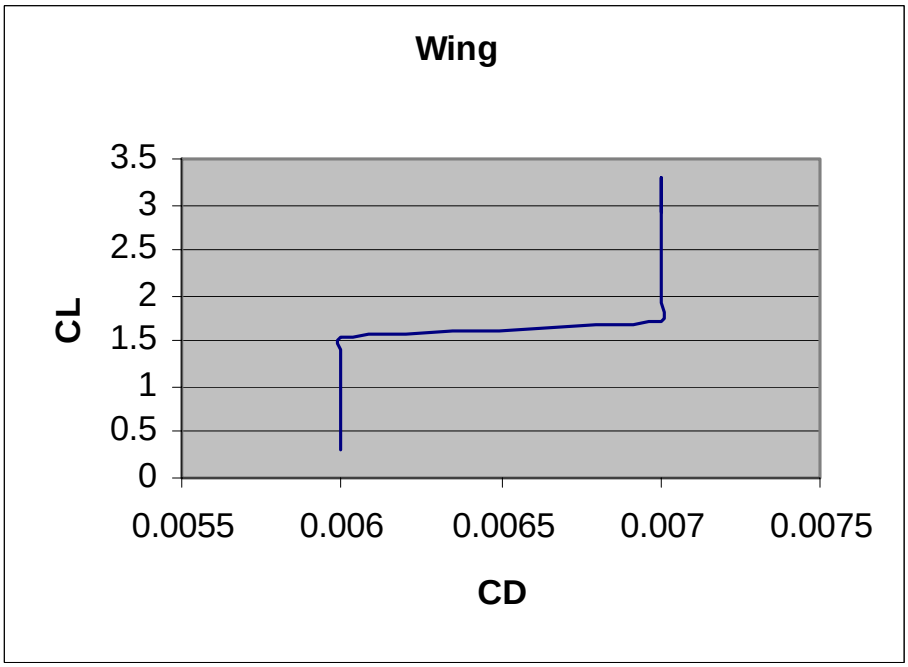

Figure 5.12 CL vs. CD (W)

The changing of C_L with C_D and calculating C_L/C_D for 2-D wing

From figure 5.12 C_D was constant and then start to increase slightly with C_L (between 1.5 and 1.8 of C_L), then returned to a constant value.

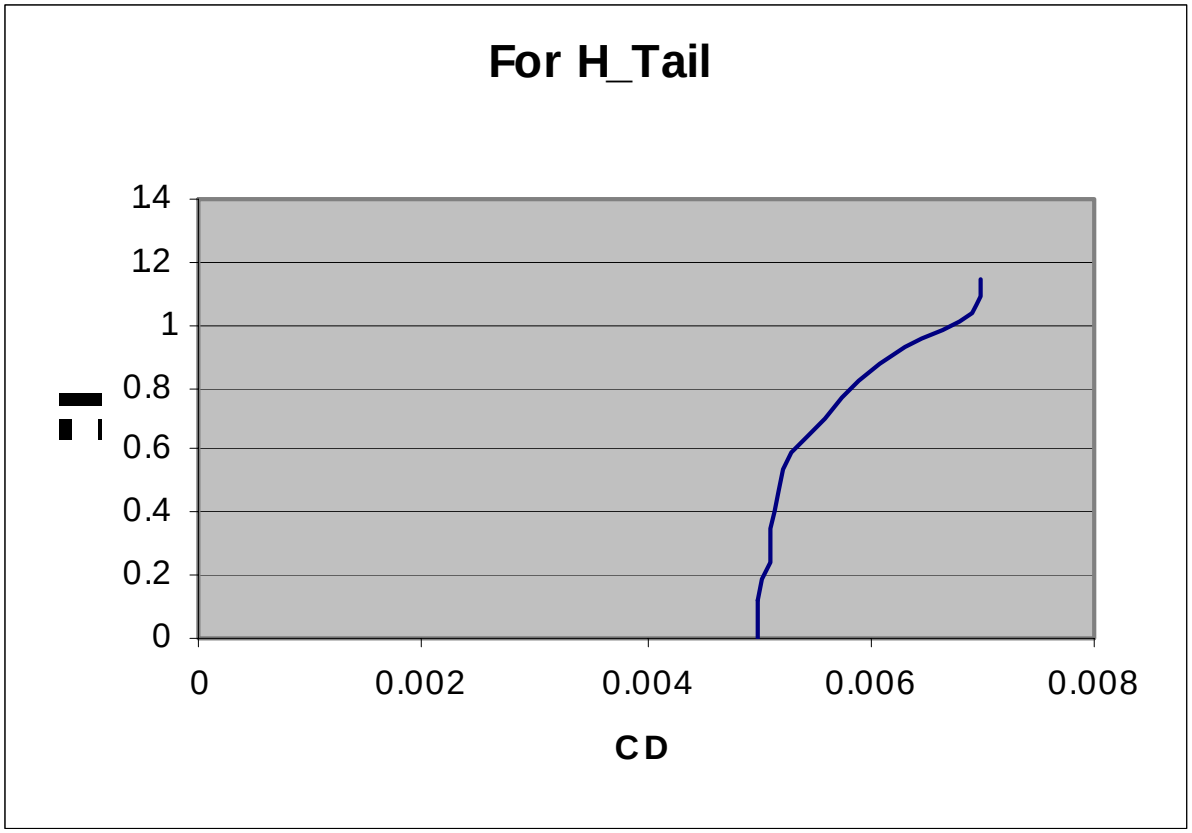

Figure 5.13 C_L vs. C_D (H-T)
The changing of CL with CD and calculating CL/CD for 2-D h-tail

At horizontal tail figure 5.13 shows that the change of C_D is started slightly at higher values of C_L.

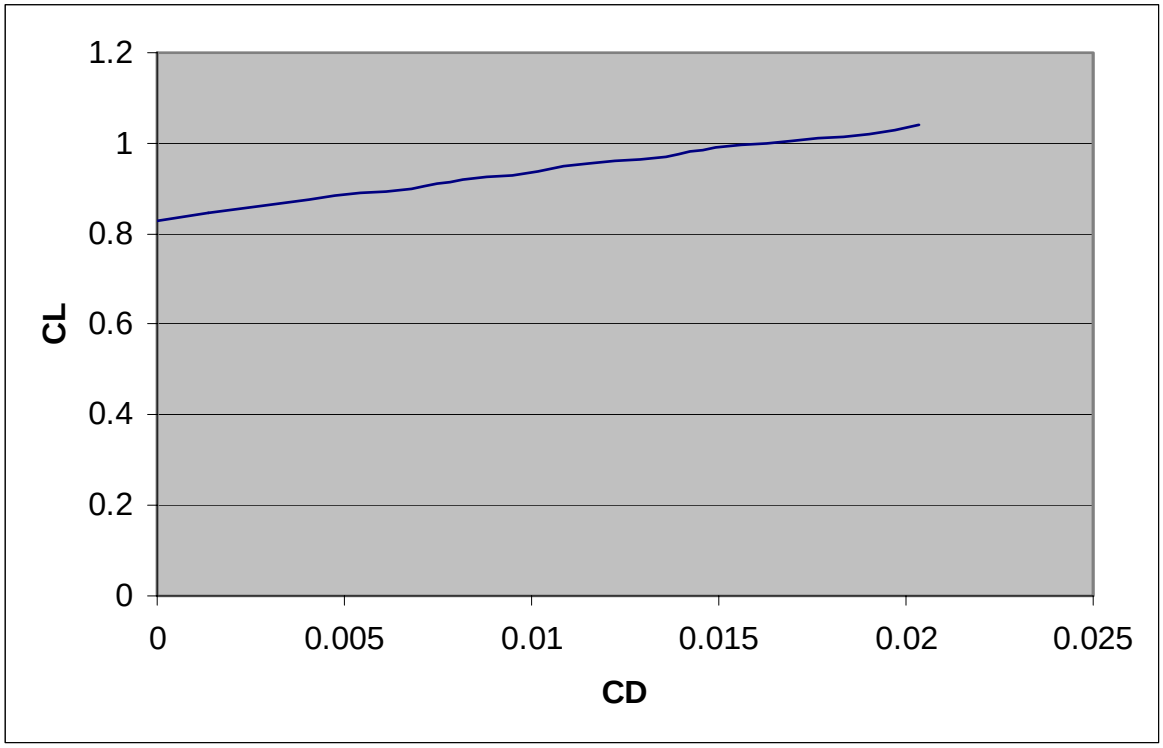

Figure 5.14 C_L vs. C_D (with flap)
The changing of CL with CD, estimating calculating CL/CD for F.H.A

With different flap hinge angle, C_L increase slightly with C_D and that clear in figure 5.14.
There for, at different situations the increasing of C_L causes few increases in C_D, which gives up higher velocity and less losing in fuel. But on flap situation it is different and that explain the using of flap during land.

6. Weight and Structure

6.1. Introduction

Before the structure can be designed, we need to determine the loads that will be imposed on the aircraft. This section deals with the general issue of aircraft loads and how they are predicted at the early stages of the design process.

Each part of the aircraft is subject to many different loads. In the final design of an aircraft structure, one might examine tens of thousands of loading conditions of which several hundred may be critical for some part of the airplane. In addition to the obvious loads such as wing bending moments due to aerodynamic lift, many other loads must be considered. These include items such as inertia relief, the weight and inertial forces that tend to reduce wing bending moments, landing loads and taxi-bump loads, pressurization cycles on the fuselage, local high pressures on floors due to high-heeled shoes, and many others.

These loads are predicted using Navier-Stokes computations, wind tunnel tests, and other simulations. Static and dynamic load tests on structural components are carried out to assure that the predicted strength can be achieved. The definition of strength requirements for commercial aircraft is specified in FAR Part 25 and this section deals with those requirements in more detail.

6.3. *V-n* Diagrams

6.3.1. Maneuver Diagram

This diagram illustrates the variation in load factor with airspeed for maneuvers. At low speeds the maximum load factor is constrained by aircraft maximum C_L. At higher speeds the maneuver load factor may be restricted as specified by FAR Part 25.

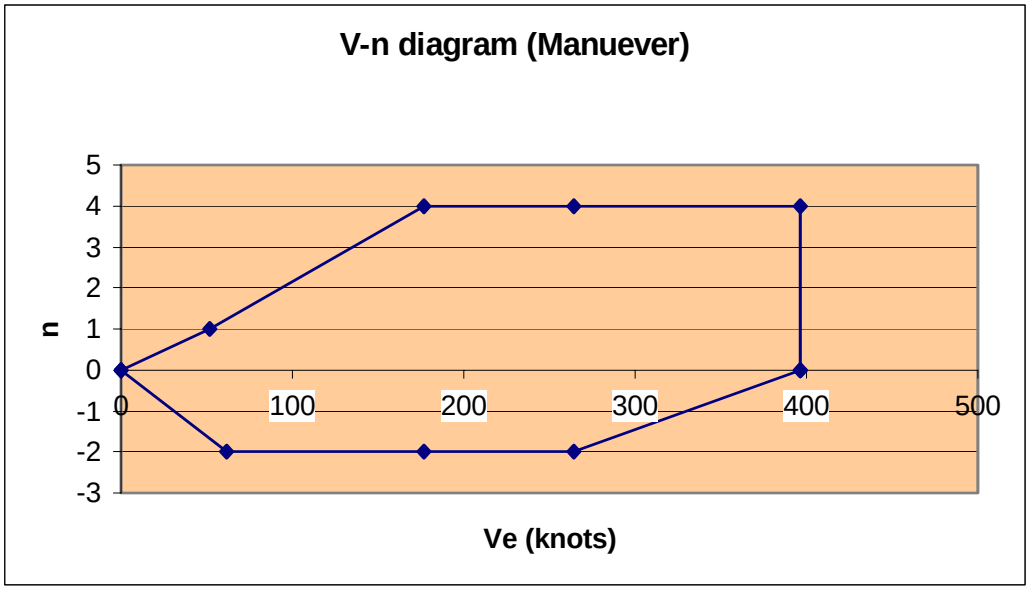

Figure 6.1 *V-n* Diagram for maneuvering

6.3.2. Gust Diagram

Loads associated with vertical gusts must also be evaluated over the range of speeds. The FAR's describe the calculation of these loads in some detail. Here is a summary of the method for constructing the V-n diagram. Because some of the speeds (e.g. V_B) are determined by the gust loads, the process may be iterative. Be careful to consider the alternative specifications for speeds such as V_B. The gust load may be computed from the expression given in FAR Part 25. This formula is the result of considering a vertical gust of specified speed and computing the resulting change in lift. The associated incremental load factor is then multiplied by a load alleviation factor that accounts primarily for the aircraft dynamics in a gust.

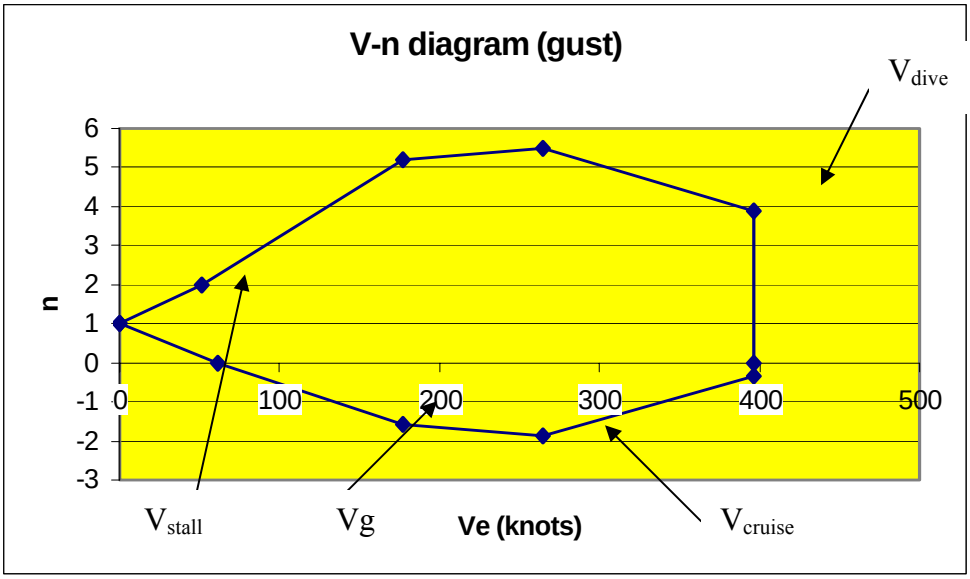

Figure 6.2 *V-n* diagram for gust

Note that:

Vg: maximum speed in turbulence. And V_{dive}: aircraft maximum speed.

Now we will make a comparison between fig 6.1 and fig 6.2 as seen below

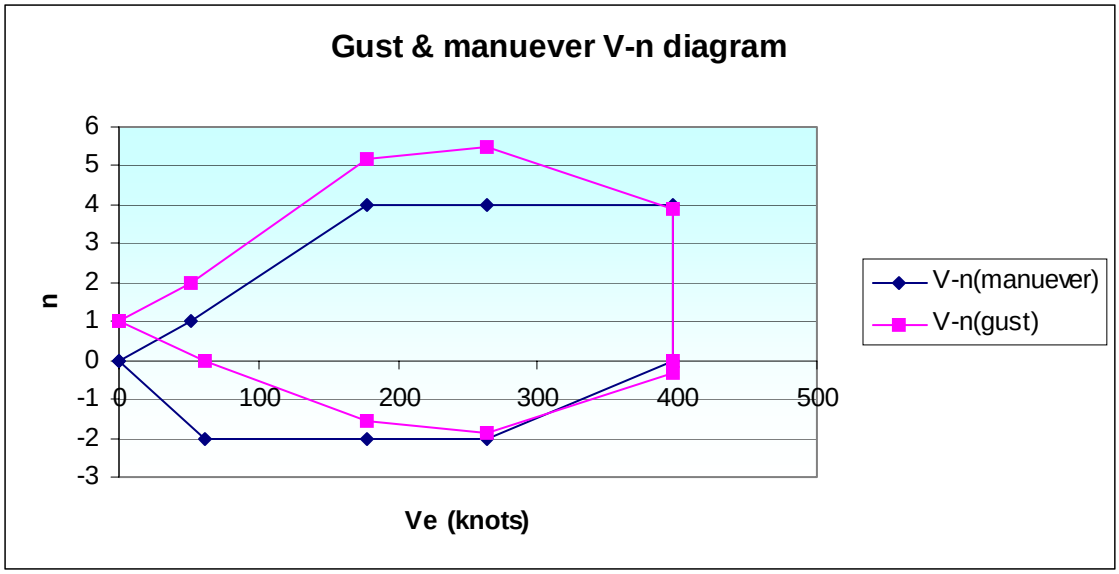

Figure 6.3 Gust and maneuvering *V-n* Diagrams

6.3.3. Combined *V-n* Diagram

The benefit of the combined *V-n* Diagram is to determine the most critical limit load factors at each speed.

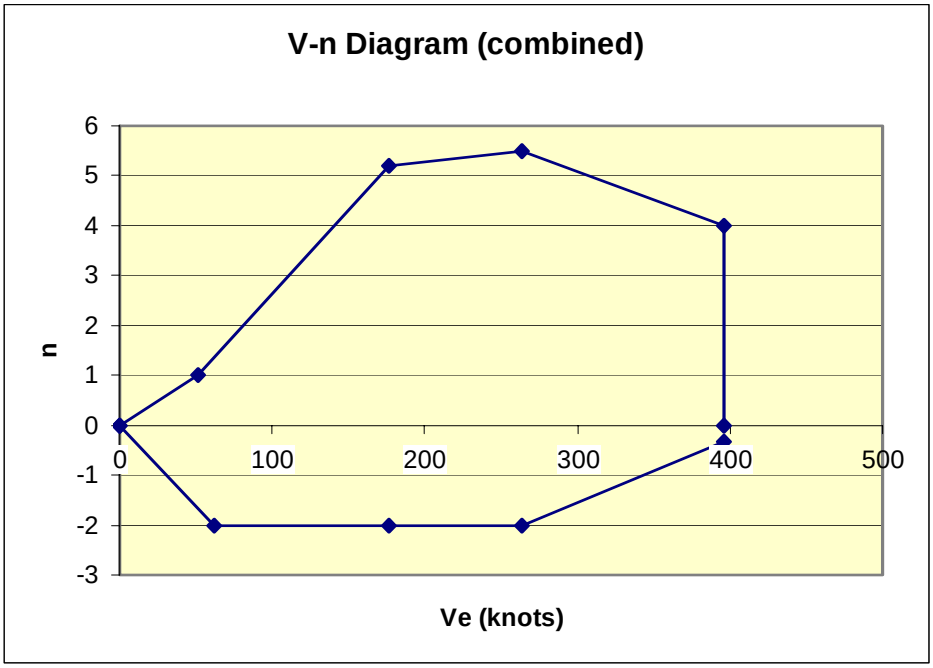

Figure 6.4 Combined *V-n* diagram

It can be seen from the Fig 6.4 that our aircraft maximum limit load factor is between 2 to 5.5 g.

6.4. Lift Distribution on the Wing

The lift distribution on the wing is calculated from the java applet that is available on:

http://adg.stanford.edu/aa241/aircraftdesign.html

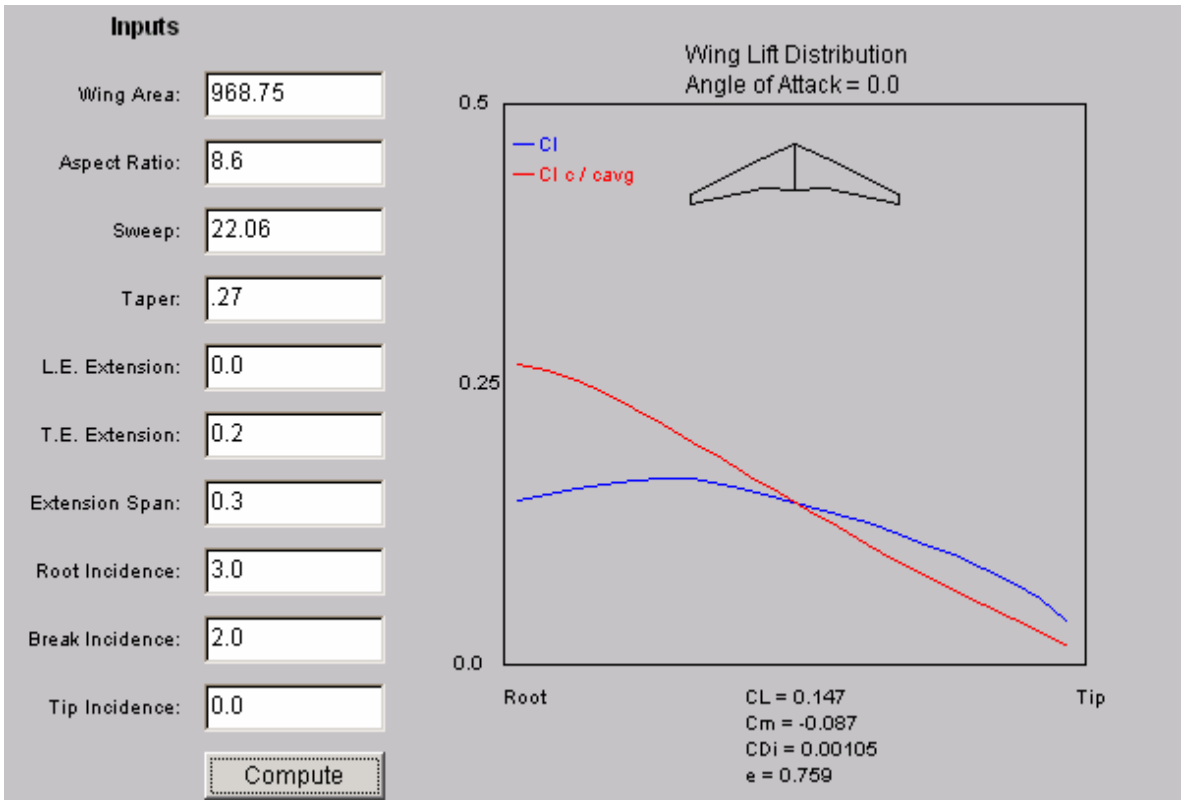

Figure 6.5 Lift & C_L distribution on the wing with extended camber

6.5. Component Weights

In the following table some of our designed aircraft components and their weights are listed:

Table 6.7 Component Weights

Component	Weight (lbm)
Wing	9848.49
Horizontal tail	311.473
Vertical tail	982.8785
Fuselage	15028.7469
Main landing gear	1471.97
Nose landing gear	252.25
Engine	2939.64
Fuel	20342
Hydraulics	268.3559
Avionics	80.9345
TOTAL	51526.7343
Designed Gross Weight	86011

It can be seen that the total weight is less than the designed gross weight because some components were not included in the calculation such as APU, electrical system, air conditioning and anti-ice, flight controls, furnishing, starter …etc

They were not calculated because of their dependency on some historical data that may not be beyond the scope of this course

6.6. Component Centers of Gravity

Note that in the following table X & Y distances are taken from the preset datum, which are the nose and the ground.

Table 6.8 Component Centers of Gravity

Component	X	Y
Wing	53.01	8.4
Horizontal tail	97.05	14.88
Vertical tail	101.39	24.16
Fuselage	29.055	11.65
Main landing gear	56.34	9.14
Nose landing gear	15.1	9.14
Engine	46.78	6.9
Fuel Tank 1	51.09	9.14
Fuel Tank 2&3	52.99	10.14
Fuel Tank 4	62.19	9.45
Whole Aircraft	53.1382	10.1997

6.7. CG Envelop Diagram

During the flight, we know that the aircraft is consuming fuel. Therefore, the weight of fuel is decreasing which leads to the variation of the center of gravity for each flight segment. The CG envelop for our aircraft during the flight segment is illustrated as follows.

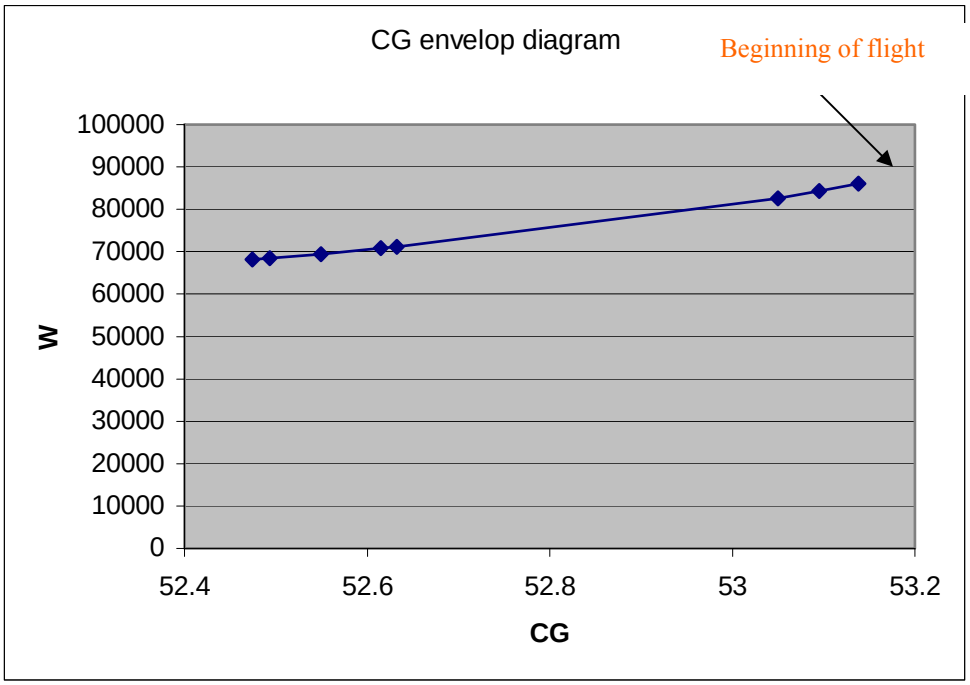

Figure 6.6 CG Envelop

It can be seen the CG envelop is simply a smoothly decreasing line because we assume that the fuel is withdrawn from each tank as the same ratio as each tank ratio to the total fuel weight. So, CG is constrained between ***52.474 ft*** and ***53.138 ft*** from the nose of aircraft.

7. Performance

7.1 Level Flight

If the aircraft is flying in uncelebrated level flight then the sum of the forces must equal zero. So the thrust equal drag and lift equal weight. These can be expressed as follows:

7.1.2 Power Available & Minimum Power required for level flight

Thrust is force, which in steady level flight equals the drag and these can be calculated as follows:

Table7.1 thrust available at level flight

Mach	Thrust, lb
0	11068.82
0.1	9800.435
0.2	8788.571
0.3	7982.409
0.4	7382.391
0.5	6886.001
0.6	6440.204
0.7	6098.256
0.8	5807.567
0.9	5619.174

Table7.2 Minimum Drag or thrust required for level flight

V, ft/s	q, psf	Sw, ft^2	CD0	(Dmin) orT_{req} lb lb
0	0	968.75	0.006	0
111.64	14.81223	968.75	0.006	172.1922228
223.28	59.24894	968.75	0.006	688.768891
334.92	133.3101	968.75	0.006	1549.730005
446.56	236.9957	968.75	0.006	2755.075564
558.2	370.3059	968.75	0.006	4304.805569
669.84	533.2404	968.75	0.006	6198.920019
781.48	725.7995	968.75	0.006	8437.418915
893.12	947.983	968.75	0.006	11020.30226
1004.76	1199.791	968.75	0.006	13947.57004

Plot of $T_{required}$ & available for level flight

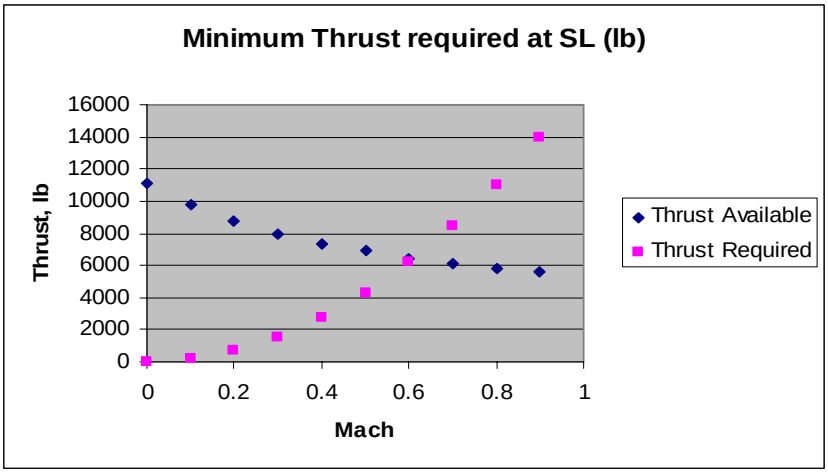

Figure7.1 $T_{required\ \&}$ available VS. Mach

Form the figure above we can find for level flight the maximum Mach number we reach is 0.6 which means that the maximum thrust required is 6440.2 lb. Also at level flight the speed for minimum thrust or drag is 351.3134 ft/s and lift coefficient is 0.4767.

7.1.2 Power Available & Minimum Power required for level flight

Power is force times velocity, which in steady level flight equals the drag times the velocity and these can be calculated as follows:

Table7.3 Power available at level flight

P aval hp	P req hp
0	0
1989.31	0.626154
3567.84	2.504614
4860.851	5.635382
5993.965	10.01846
6988.665	15.65384
7843.466	22.54153
8664.845	30.68152
9430.644	40.07383
10265.31	50.71844

- Plot of minimum $P_{required}$ & Available $_{for}$ level flight

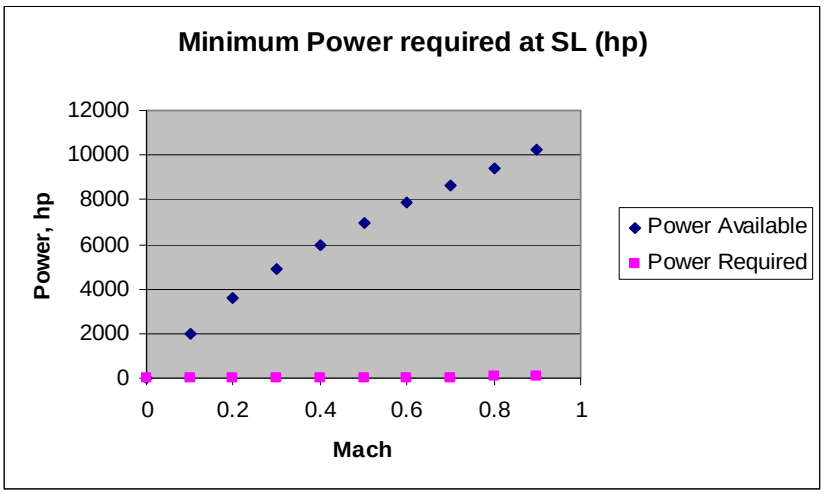

Figure7.2 Minimum $P_{required}$ & Available VS. Mach

From the figure shown above the we can say that we have power available much grater than power required and our velocity at minimum power is 266.94 ft/s which is about 0.76 times the velocity for minimum thrust and the lift coefficient is 0.8257 which is about 73% higher than the lift coefficient for minimum drag.

7.2 Cruise Limit

In this section we will steady the thrust and power at cruise altitude which is about 36 k ft and as we know our mach number is 0.82

7.2.1 Thrust available and required for cruise altitudes = 36 k ft

Table 7.4 Thrust available for cruise altitudes = 36 k ft

Mach	Thrust, lb
0	3346.696
0.1	2952.38
0.2	2713.393
0.3	2525
0.4	2440.456
0.5	2406.506
0.6	2424.701
0.7	2442.231
0.8	2615.757
0.9	2736.915

Table 7.5 Minimum thrust required for cruise altitudes = 36 k ft

V, ft/s	q, psf	Sw, ft^2	CD0	(Dmin) orTreq
0	0	968.75	0.006	0
96.87	3.332655	968.75	0.006	38.74211983
193.74	13.33062	968.75	0.006	154.9684793
290.61	29.9939	968.75	0.006	348.6790784
387.48	53.32249	968.75	0.006	619.8739172
484.35	83.31639	968.75	0.006	968.5529957
581.22	119.9756	968.75	0.006	1394.716314
678.09	163.3001	968.75	0.006	1898.363872
774.96	213.29	968.75	0.006	2479.495669
871.83	269.9451	968.75	0.006	3138.111706

- Plot of $T_{required}$ & available for cruise altitudes = 36 k ft

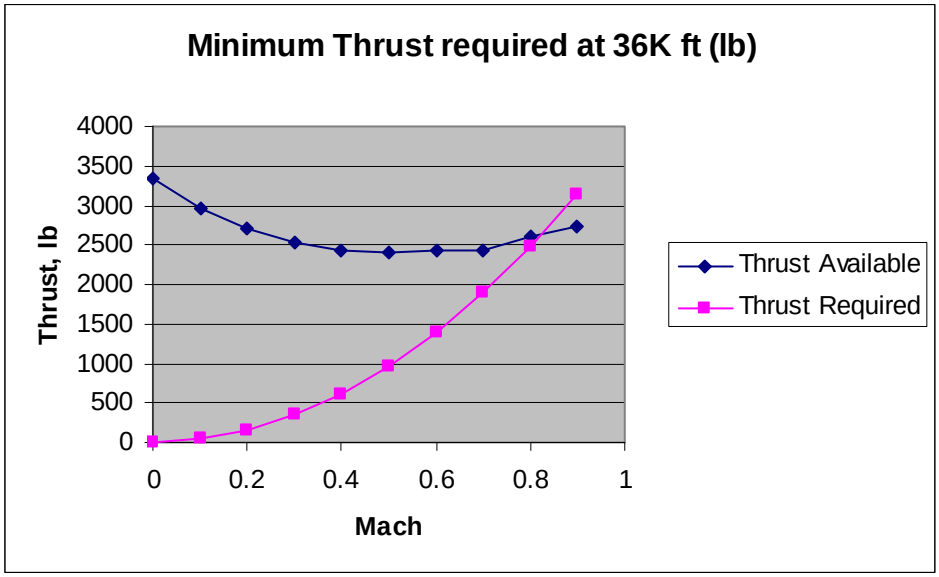

Figure7.3 $T_{required}$ & available VS. Mach

From the figure above we can find that at Mach 8.2 the thrust required is about 2600lb while the thrust available at the same speed is about 2650 lb as well.

7. 2.2 Power available & Minimum Power required for cruise altitudes = 36 k ft

In this case we will calculate the power required and available in the same way that we did before as follows:

Table 7.6 Power available& Minimum Power required for cruise altitudes = 36 k ft

Pavl	Preq
0	0
519.9945	0.14088
955.8051	0.563522
1334.164	1.267924
1719.324	2.254087
2119.256	3.522011
2562.336	5.071696
3011.005	6.903141
3685.649	9.016348
4338.408	11.41132

- Plot of minimum P $_{required}$ & available power for cruise altitudes = 36 k ft

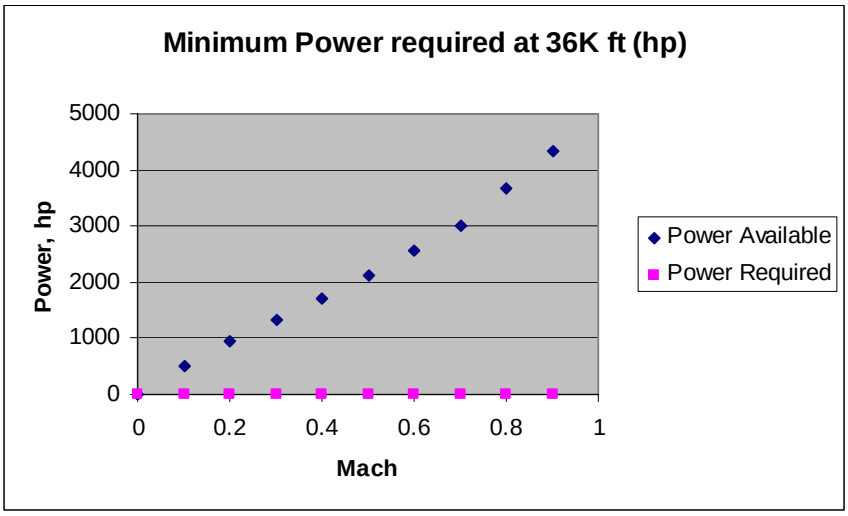

Figure7.4 Minimum P $_{required}$ & Available VS. Mach

As we see from the figure above that we have at Mach 0.82 power available about 3700 hp while the minimum required power at the same Mach number is only 9.4 hp.

7.3 Optimum Range

Here we will calculate the best minimum thrust and velocity and lift coefficient.

7.3.1 Thrust required and available for best range for level flight

Thrust required and available for best range for level flight can calculate as follows:

Table7.7 Thrust required and available for best range for level flight

V, ft/s	q, psf	Sw, ft^2	CD0	(Dmin) orTreq lb
0	0	968.75	0.006	0
111.64	14.81223	968.75	0.006	114.7948152
223.28	59.24894	968.75	0.006	459.1792607
334.92	133.3101	968.75	0.006	1033.153337
446.56	236.9957	968.75	0.006	1836.717043
558.2	370.3059	968.75	0.006	2869.870379
669.84	533.2404	968.75	0.006	4132.613346
781.48	725.7995	968.75	0.006	5624.945943
893.12	947.983	968.75	0.006	7346.868171
1004.76	1199.791	968.75	0.006	9298.380029

- Plot of thrust available and required for best range:

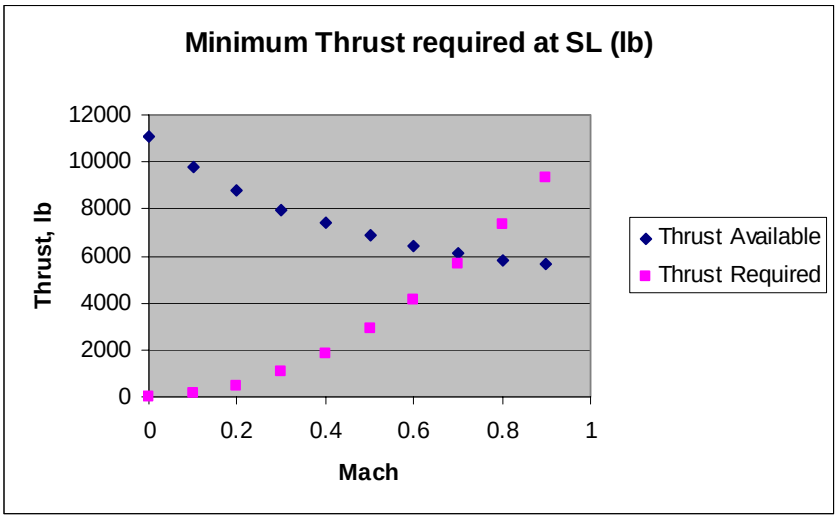

Figure7.5 T $_{required\ \&}$ available VS. Mach

From the figure above we can say that the best range where the Mach number equals 0.7 and the thrust will be 5624.5 lb .Also in this case the speed for best range is 462.35 ft/s and lift coefficient is 0.0073.

7.3.2 Thrust required and available for best range for cruise altitudes = 36 k ft

In the same way we will calculate thrust required and available for best range but with cruise altitude as follows:

Table7.8 Thrust required and available for best range for cruise altitudes = 36 k ft

V, ft/s	q, psf	Sw, ft^2	CD0	(Dmin) orTreq
0	0	968.75	0.006	0
96.87	3.332655	968.75	0.006	25.82807989
193.74	13.33062	968.75	0.006	103.3123195
290.61	29.9939	968.75	0.006	232.452719
387.48	53.32249	968.75	0.006	413.2492782
484.35	83.31639	968.75	0.006	645.7019971
581.22	119.9756	968.75	0.006	929.8108759
678.09	163.3001	968.75	0.006	1265.575914
774.96	213.29	968.75	0.006	1652.997113
871.83	269.9451	968.75	0.006	2092.074471

- Plot of Thrust required and available for best rang for cruise altitudes = 36 k ft.

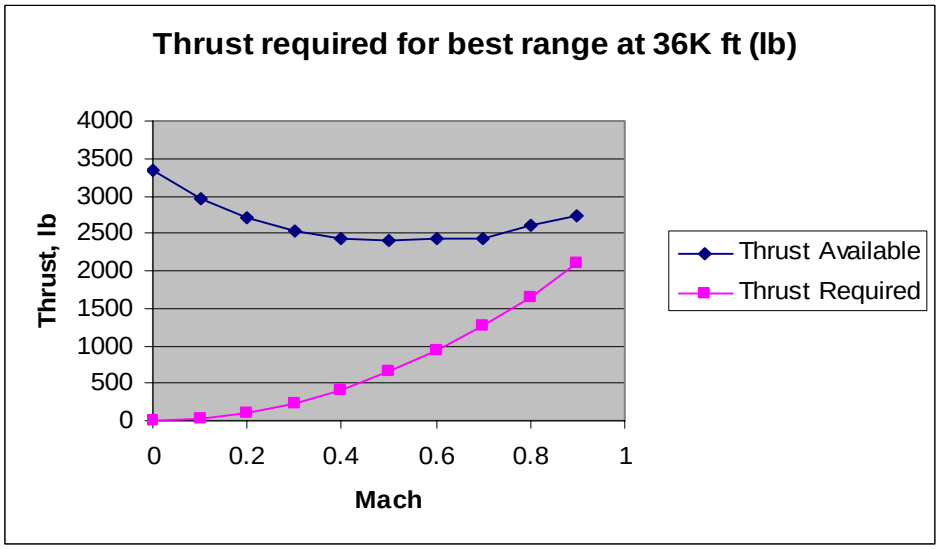

Figure7.6 $T_{required\ \&}$ available VS. Mach

For cruise at Mach 0.82, there is extra thrust available. This suggests that a partial thrust setting is required and the TSFC will correspond to that partial throttle setting. Therefore for best range at M=0.82 thrust required =1750 lb and throttle setting (1750/2525) is 0.693 from the partial throttle setting of 70% at 36 kft and M=0.82, the TSFC (0.75*0.22) is 0.165(1/hr) for best cruise range.

Since we have used TSFC=0.5(1/hr) in cruise analysis, it suggests that we have enough fuel for (1500 n.m*0.5) 4545 n.m.

7.4. Operating Envelop (P_S for n=1)

The aircraft operating envelop or flight envelops maps the combination of altitude and velocity that aircraft has been designed to withstand. The level flight operating envelope is determined from the P_S=0.Typically the operating envelops is calculated at takeoff weight, cruise weight or combater weight.

The following figure will show our operating envelop at n=1

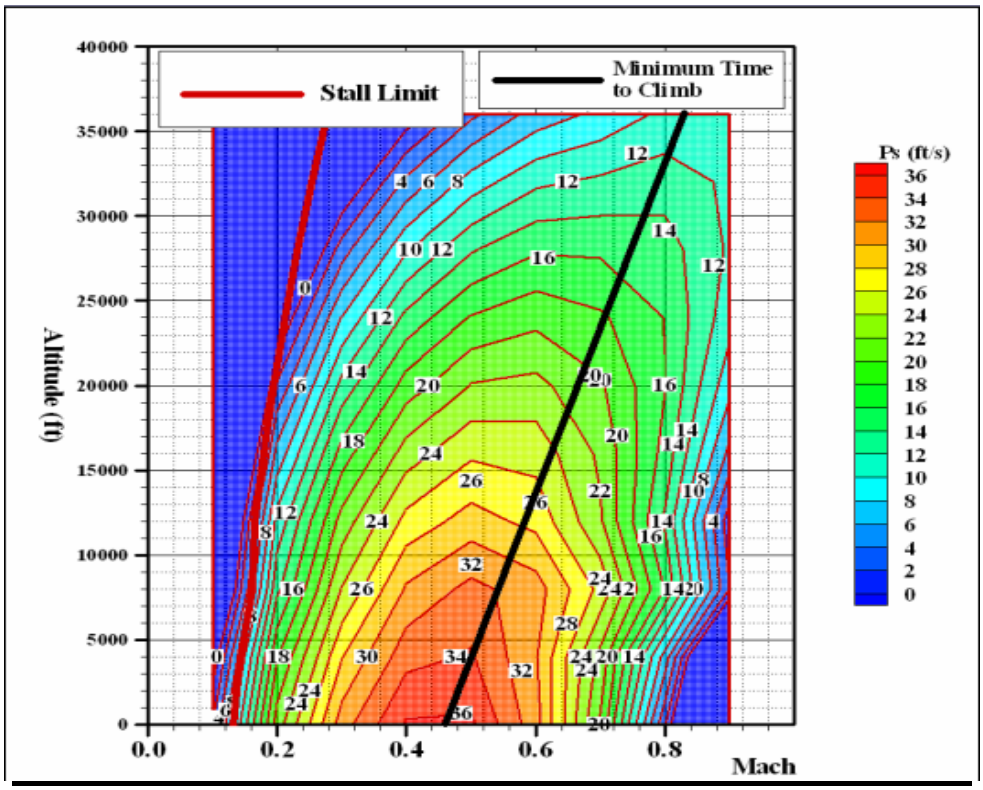

Figure7.7 Mach vs. altitude ft

From the figure above we see that the stall limit start at Mach number about 0.13 at SL and reach to about 0.24 at cruise altitude 36 k ft . Also the minimum time to climb trajectory starts at approximately Mach 0.44 at SL and reaches to about 0.82 at cruise altitude.

7.5 Takeoff Analysis

The takeoff analysis of the aircraft can be shown in illustrated figure .the ground roll includes tow parts –the level ground roll and the ground roll during rotation to the angle of the angle of attack for lift off. After rotation the aircraft follows an approximately circular arc which is called transition until it reaches the climb angle.

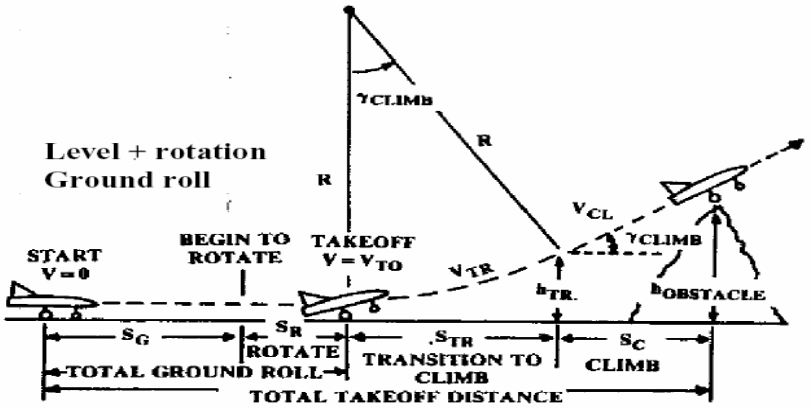

Figure 7.8 Takeoff analysis

- **Total Takeoff Distance**

For our aircraft we have the following

1. Ground roll S_G = **1.725 ft**
2. Ground roll distance during rotation S_R = **514.8 ft**
3. Transition S_{TR} =**1448 ft**
4. Climb S_C = **589.0654 ft**

So the total length = 4277 ft = 1.3 km

- **Balance Field Length**

The balance field length is the total distant including obstacle clearance when an engine fails, so for our aircraft

BFL = 13971 ft = 4.1 km

So from the above, when we compare between BFL and total takeoff distance we need 3 times total length for tacking off.

8. Stability and Control

An understanding of the important stability and control design parameters can be attained through study of simpler method. The basic concept of stability is simply when air craft disturbed it tends to return to its equilibrium position.

In this project we will concentrate in trim analysis, so that we will calculate the following

- **Moment coefficient:**

1. Pitching moment for the wing

$C_{mw} = -0.0326$

2. Pitching moment contribution of the fuselage and nacelles

$C_{m\alpha fus} = 0.0308$

3. Pitching moment increment due to flap deflection

$C_{mw\delta f} = 0$ assumption

- **Center of gravity**

    1. $X_{cg} = 53.955$ ft (from the nose)

- **Aerodynamic center for:**

    1. Wing $X_{acw} = 51.22$ ft

    2. Horizontal tail $X_{ach} = 96.01$ ft

8.1. Trim Analysis

For trim analysis we have to calculate total lift coefficient and pitching moment so that we have the following:

- Calculating the total lift coefficient $C_{L,total}$

  By assuming air craft angles of attack and elevator deflection angles (δ_E), We can calculate the total lift coefficient by the following

  1. calculating $\mathbf{C_{Lh}}$, $\mathbf{C_{L\ total}}$ and $\mathbf{C_{mcg}}$ **from Eq.16.7, 16.29,16.30 of Ref.4**

     - $C_{L\alpha h} = 0.14$
     - Iw = 0
     - ih= 0
     - Change in zero lift angle due to plain flap:

     $(\Delta\alpha_{OL}) = -1.4118*\delta_f$ (Eq. 16.14, 16.15 of Ref.4

     - Downwash $(\partial\varepsilon/\partial\alpha) = 1$ which is the most effected ratio

     - **When α changing from 0-10^o and δ_E = -0.25**

$\mathbf{C_{L\ total}}$	-0.0108	0.1266	0.2640	0.4015	0.5389	0.6763
$\mathbf{C_{mcg}}$	0.0344	0.0105	-0.0134	-0.0373	-0.0612	-0.0851

     - **When α changing from 0-10^o and δ_E = 0**

$\mathbf{C_{L\ total}}$	0	0.1374	0.2749	0.4123	0.5497	0.6872
$\mathbf{C_{mcg}}$	-0.0015	-0.0254	-0.0493	-0.0732	-0.0971	-0.1210

     - **When α changing from 0-10^o and δ_E = 0.25**

$\mathbf{C_{L\ total}}$	0.0108	0.1483	0.2857	0.4231	0.5605	0.6980
$\mathbf{C_{mcg}}$	-0.0401	-0.0640	-0.0879	-0.1118	-0.1357	-0.1596

Plot of $C_{mcg\ vs.}$ $C_{L\ total}$

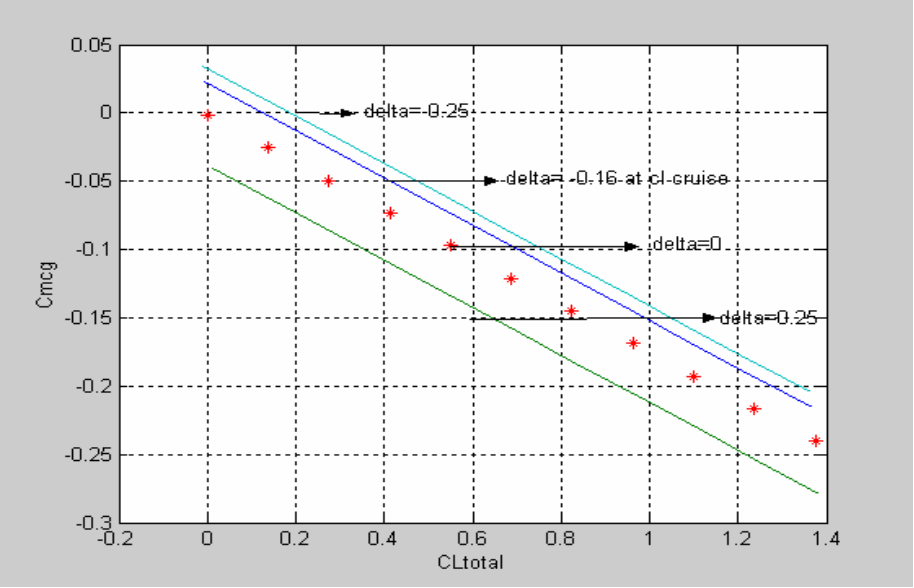

Figure 8.1 C_{mcg} vs. $C_{L\ total}$

From the figure above we see for trim analysis the elevator angle is between -0.25 and 0.25, also at C_L cruise 0.12 we have the following

We can get at C_L cruise =0.12 that δ_E = -0.16

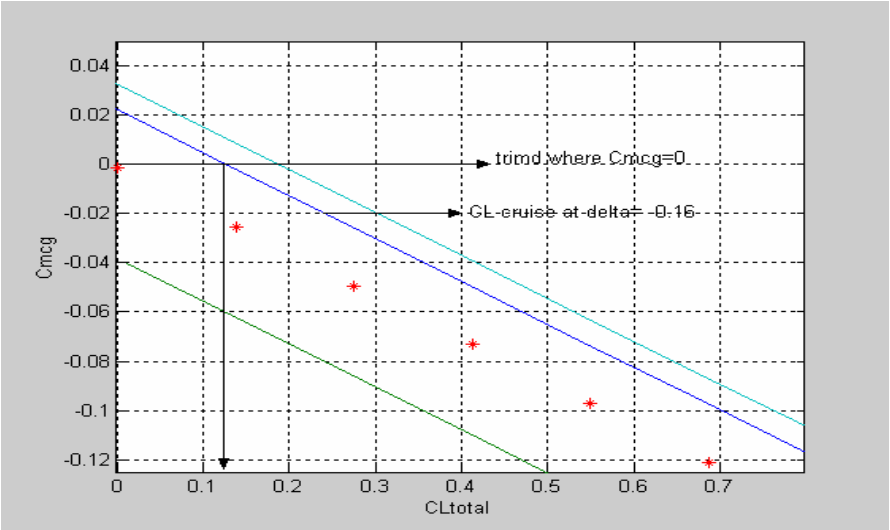

Figure 8.2 C_{mcg} vs. $C_{L\ total}$

From the figure above the elevator angle δ_E = -0.16

The elevator deflection for trim can be found by interpolating for $Cm_{c,g} = 0$

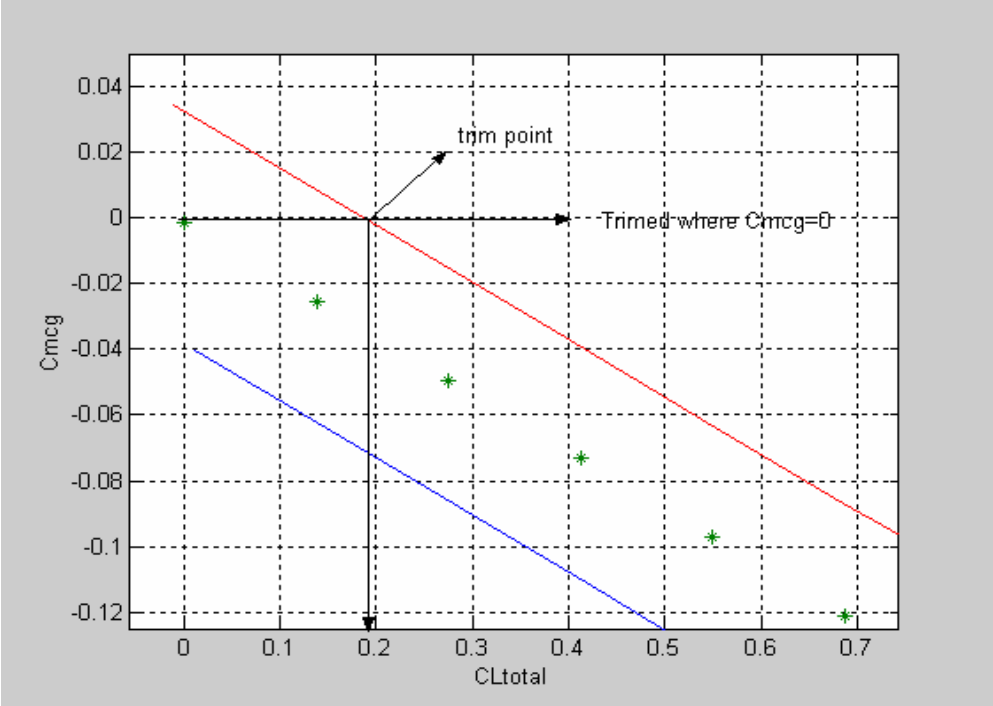

Figure8.3 $Cm_{c,g}$ vs. CL total

We can conclude that at $\mathbf{C_{m,cg}} = 0$

δ_E	$C_{L\ total}$
0	0
-0.25	0.19
-0.16	0.12 ($C_{Lcruise}$)

So we can say that our aircraft is stable.

8.2. Trim drag for the total induced drag

The trim drag for the total induced can be calculated from (Eq.16.31 of Ref.4) and based on C_L cruise=0.12 we found
$C_{Di\ trimmed}$ = 0.00049112

When we compare this value and the C_{Do}=0.006 it is very small

9. Advance Technology Consideration

9.1. Structure

9.1.1. Composites and Advanced Materials

“ For many years, aircraft designers could propose theoretical designs that they could not build because the materials needed to construct them did not exist. (The term "unobtainium" is sometimes used to identify materials that are desired but not yet available.) For instance, large space planes like the Space Shuttle would have proven extremely difficult, if not impossible, to build without heat-resistant ceramic tiles to protect them during reentry. And high-speed forward-swept-wing airplanes like Grumman's experimental X-29 or the Russian Sukhoi S-27 Berkut would not have been possible without the development of composite materials to keep their wings from bending out of shape.

Composites are the most important materials to be adapted for aviation since the use of aluminum in the 1920s. Composites are materials that are combinations of two or more organic or inorganic components. One material serves as a "matrix," which is the material that holds everything together, while the other material serves as reinforcement, in the form of fibers embedded in the matrix. Until recently, the most common matrix materials were "thermosetting" materials such as epoxy, bismaleimide, or polyimide. The reinforcing materials can be glass fiber, boron fiber, carbon fiber, or other more exotic mixtures.

Fiberglass is the most common composite material, and consists of glass fibers embedded in a resin matrix. Fiberglass was first used widely in the 1950s for boats and automobiles, and today most cars have fiberglass bumpers covering a steel frame. Fiberglass was first used in the Boeing 707 passenger jet in the 1950s, where it comprised about two percent of the structure. By the 1960s, other composite materials became available, in particular boron fiber and graphite, embedded in epoxy resins. The U.S. Air Force and U.S. Navy began research into using these materials for aircraft control surfaces like ailerons and rudders. The first major military production use of boron fiber was for the horizontal stabilizers

on the Navy's F-14 Tomcat interceptor. By 1981, the British Aerospace-McDonnell Douglas AV-8B Harrier flew with over 25 percent of its structure made of composite materials.

Making composite structures is more complex than manufacturing most metal structures. To make a composite structure, the composite material, in tape or fabric form, is laid out and put in a mold under heat and pressure. The resin matrix material flows and when the heat is removed, it solidifies. It can be formed into various shapes. In some cases, the fibers are wound tightly to increase strength. One useful feature of composites is that they can be layered, with the fibers in each layer running in a different direction. This allows materials engineers to design structures that behave in certain ways. For instance, they can design a structure that will bend in one direction, but not another. The designers of the Grumman X-29 experimental plane used this attribute of composite materials to design forward-swept wings that did not bend up at the tips like metal wings of the same shape would have bent in flight.

The greatest value of composite materials is that they can be both lightweight and strong. The heavier an aircraft weighs, the more fuel it burns, so reducing weight is important to aeronautical engineers.

Despite their strength and low weight, composites have not been a miracle solution for aircraft structures. Composites are hard to inspect for flaws. Some of them absorb moisture. Most importantly, they can be expensive, primarily because they are labor intensive and often require complex and expensive fabrication machines. Aluminum, by contrast, is easy to manufacture and repair. Anyone who has ever gotten into a minor car accident has learned that dented metal can be hammered back into shape, but a crunched fiberglass bumper has to be completely replaced. The same is true for many composite materials used in aviation.

Modern airliners use significant amounts of composites to achieve lighter weight. About ten percent of the structural weight of the Boeing 777, for instance, is composite material. Modern military aircraft, such as the F-22, use composites for at least a third of their structures, and some experts have predicted that future military aircraft will be more than two-thirds composite materials. But for now, military aircraft use substantially greater percentages of composite materials than commercial passenger aircraft primarily because of the different ways that commercial and military aircraft are maintained.

Aluminum is a very tolerant material and can take a great deal of punishment before it fails. It can be dented or punctured and still hold together. Composites are not like this. If they are damaged, they require immediate repair, which is difficult and expensive. An airplane made entirely from aluminum can be repaired almost anywhere. This is not the case for composite materials, particularly as they use different and more exotic materials. Because of this, composites will probably always be used more in military aircraft, which are constantly being maintained, than in commercial aircraft, which have to require less maintenance.

Thermoplastics are a relatively new material that is replacing thermo sets as the matrix material for composites. They hold much promise for aviation applications. One of their big advantages is that they are easy to produce. They are also more durable and tougher than thermo sets, particularly for light impacts, such as when a wrench dropped on a wing accidentally. The wrench could easily crack a thermo set material but would bounce off a thermoplastic composite material.

In addition to composites, other advanced materials are under development for aviation. During the 1980s, many aircraft designers became enthusiastic about ceramics, which seemed particularly promising for lightweight jet engines, because they could tolerate hotter temperatures than conventional metals. But their brittleness and difficulty to manufacture were major drawbacks, and research on ceramics for many aviation applications decreased by the 1990s.

Aluminum still remains a remarkably useful material for aircraft structures and metallurgists have worked hard to develop better aluminum alloys (a mixture of aluminum and other materials). In particular, aluminum-lithium is the most successful of these alloys. It is approximately ten percent lighter than standard aluminum. Beginning in the later 1990s it was used for the Space Shuttle's large External Tank in order to reduce weight and enable the shuttle to carry more payloads. Its adoption by commercial aircraft manufacturers has been slower; however, due to the expense of lithium and the greater difficulty of using aluminum-lithium (in particular, it requires much care during welding). But it is likely that aluminum-lithium will eventually become a widely used material for both commercial and military aircraft".

SOURCE: "http://www.centennialofflight.gov"

9.1.2 Latest news on composite materials "ADVANCED TECHNOLOGY"

" Toray Industries, Inc. has agreed with Boeing Inc. of the U.S. for the supply of carbon fiber composite materials to be used in the primary structural elements of the B7E7 Dreamliner, a next-generation medium-size aircraft scheduled to enter service in 2008. Based on the agreement, Toray is to supply carbon fiber composite materials to Boeing from 2004 through 2021, total 18 years.

Figure 9.1 Boeing 7E7

During the period, Toray will provide Boeing with carbon fiber prepreg, a sheet made from epoxy resin pregnated in carbon fiber. The total value of the supply is estimated to reach approximately 3 billion US dollars. This figure will increase still further if another composite material gets approval from Boeing. Boeing has selected Toray as the sole supplier of carbon fiber reinforced plastics for the primary structures of the B7E7 aircraft. In 1982, Boeing adopted Toray's carbon fiber "TORAYCA" for the secondary structural elements of its B757 and B767, and since 1992 has been using "TORAYCA" prepreg for the primary structural elements of B777. These have been decisive factors in Boeing's project that Boeing's high evaluation for the superior performance of "TORAYCA" carbon fiber and "TORAYCA" prepreg, as well as the two companies' long reliable business relationship. The B7E7 Dreamliner is being described as an "All Composite Airplane." Based on the "Point to Point" carrier concept, which allows an airplane to offer passengers non-stop travel between destinations, the B7E7 is now undergoing development for the aims of improved fuel efficiency and extended flight range through weight reduction. Energy-saving through incorporation of a lighter fuselage is the most important factor, and the fuselage of the B7E7 is expected to make extensive use of light-weight, strong and highly durable advanced composite materials. "TORAYCA" prepreg, which is a combination of Toray-developed high-strengthened carbon fiber "TORAYCA" and toughened epoxy resin, has been used for the primary structural areas of the B777 empennage and floor beams. Boeing has selected Toray's advanced composite materials for almost all primary structural parts of the B7E7, including wing and fuselage. Accordingly, in comparison with existing airplanes, the B7E7 will incorporate a substantially increased quantity of carbon fiber composite materials.

In line with the material approval and long-term supply agreement with Boeing, Toray Composites (America), Inc. (TCA), Toray's prepreg manufacturing and marketing base in the U.S., will supply Boeing with "TORAYCA" prepreg. Prior to this, with approximately 16 billion yens of strategic investments, Toray had

proactively decided to expand production facilities of PAN-based carbon fiber and prepreg in the U.S. to meet the requirements of operations scheduled for the beginning of 2006. Toray Carbon Fibers America, Inc. (CFA), Toray's carbon fiber production base, will build a new production facility for PAN precursor, a raw material of carbon fiber, and double the size of its production facility for carbon fiber, while TCA will double its production facility for prepreg, thus enabling the company to establish an integrated production system from PAN precursor to prepreg. In France, Toray has invested about 8 billion yen in the projects for increasing production capacity for carbon fiber at SOFICAR, and at the same time increasing production capacity for PAN precursor at the Ehime Plant, with the intention to capture the growing demand for carbon fiber products globally. Both the French and Japanese new facilities are scheduled to come on stream in October 2004.

Toray started implementation of its new mid-term management reform program "Project NT - II" in April 2004. As part of the program, the company is focusing on "Expanding Advanced Materials Businesses," "Expanding and Reinforcing Global No.1 Businesses" and "Expanding Overseas Businesses." Among the strategic businesses, the carbon fiber composite material business is a core activity for the company. On the basis of the agreement with Boeing, Toray will further strengthen its partnership and the leading power of carbon fiber manufacturer based on the managerial framework of a global operation system comprising production bases in Japan, the U.S. and Europe". *By JAMES WALLAE, SEATTLE POST-INTELLIGENCER AEROSPACE REPORTER.*

9.2. Winglets “ADVANCED TECHNOLOGY”

Winglets are wing tip extensions which provide several benefits to airplane operators. Some of these benefits are listed as follows.

1. IMPROVED TAKEOFF PERFORMANCE.
2. REDUCED ENGINE MAINTENANCE COSTS
3. FUEL SAVINGS.
4. INCREASED PAYLOAD RANGE
5. ENVIRONMENTALLY FRIENDLY.
6. IMPROVED OPERATIONAL FLEXIBILITY.
7. MODERN DRAMATIC APPEARANCE (decoration).

Winglets can affect the performance of aircraft and those effects are:

- 4-5% cruise drag reduction.
- No change to stall speeds.
- When flaps are down, the lift increases.
- Significant drag reduction for take off flaps.

Figure 9.2 Winglet performance

10. Cost Analysis

10.1 Introduction:

The purchase for a civil aircraft is set to recover the RDT&E and production costs, including a fair profit. Also operation and maintenance O&M covers fuel, oil, aircrew, maintenance, and various indirect costs. This chapter will discuss the aircraft market survey and will also discuss the cost analysis of our aircraft using the modified DAPCA IV Cost Model.

10.2. Regional Market Forecast

10.2.1. Methodology

The forecast is technically a merged “top-down” and “bottom-up” view of the market. The “top-down” forecast is driven by economic models while the “bottom-up” forecast is based on an expert airline-by-airline Assessment of the market. The market forecast is primarily driven by econometric models based on historical and regional economic inputs. These models predict growth rates for the market and, when combined with existing fleets and Retirement assumptions produce a seat demand requirement. Regional Seat split models are employed to forecast units by capacity segment The results of the top-down econometric model are then tested against Nearer term anticipated fleet decisions by individual airlines. This “bottom up” Check is more useful in the near term and may result in a shift forward or backwards of the expected timing of deliveries predicted by the top down Model. = Purchasing an aircraft is, without a doubt, sometimes complex and very specialized. With so many types of aircraft to choose from based on an individual's or company's mission, figuring out an accurate bottom line cost can be an equally daunting task. Many buyers, although well-heeled and sophisticated, find out they could have saved money had they done their homework.

Table 10.1 aircraft types by seat category

Type	Class	Typical Seating	Manufacture Period
100-119 Seats			
Aerospatiale/BAe Concorde	Jet	100	1969-1979
Airbus A-318	Jet	106	2002-
Boeing B-717-200	Jet	117	1998-
Boeing B-727-100	Jet	118	1963-1970
Boeing B-737-200/200 Adv.	Jet	110	1967-1988
Boeing B-737-500	Jet	110	1989-1999
Boeing B-737-600	Jet	103	1997-
Convair CV-880	Jet	100	1959-1964
Convair CV-990	Jet	115	1961-1964
Douglas DC-9-30	Jet	100	1966-1981
Douglas DC-9-40	Jet	112	1967-1979
Douglas DC-9-87/MD-87	Jet	110	1987-1996
Embraer 195	Jet	108	2004-
Fokker F-28 Mk 0100 (Fokker 100)	Jet	100	1987-1996
Hawker Siddeley/BAe HS.121 Trident 1/2	Jet	119	1961-1984
Sud Aviation Super Caravelle 10B	Jet	114	1964-1969
Sud Aviation Caravelle 11	Jet	100	1967-1968
Fairchild Dornier 928	Jet	100	2005-

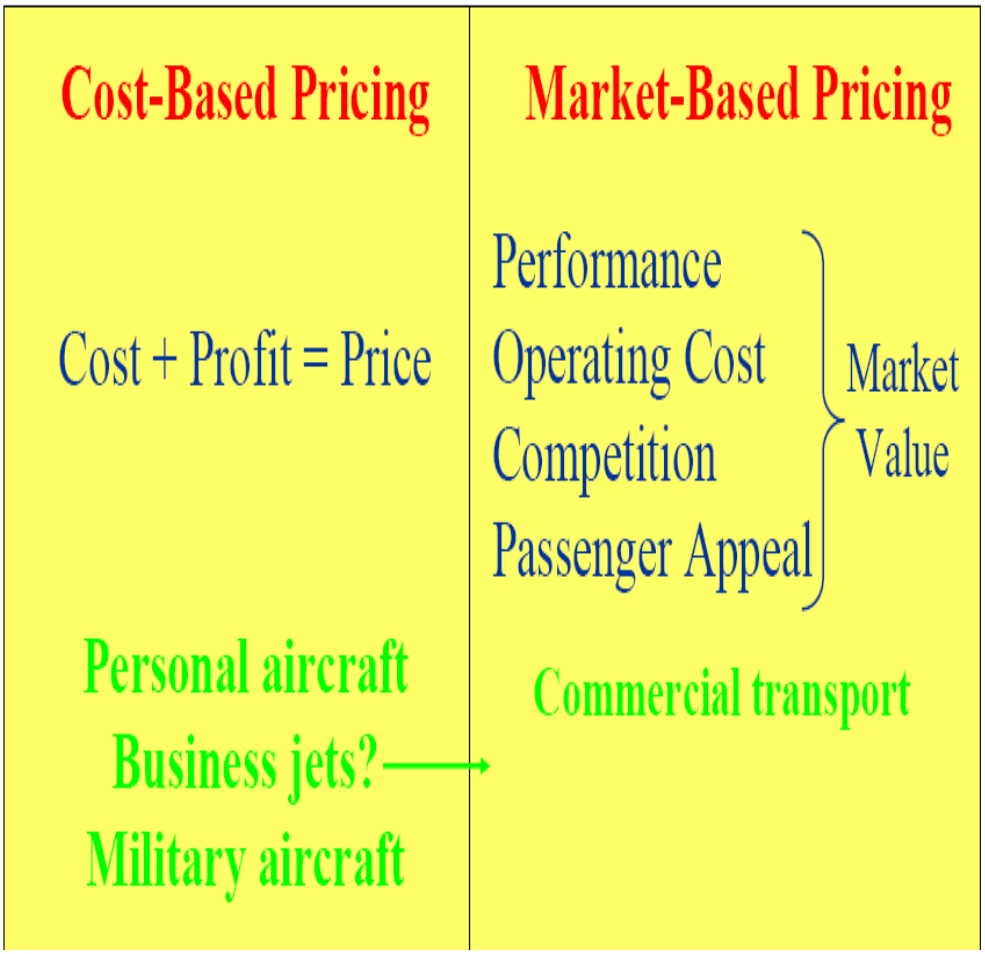

Figure (10.1) Aircraft Pricing and Aircraft Types by Seat Category

Regional Routes

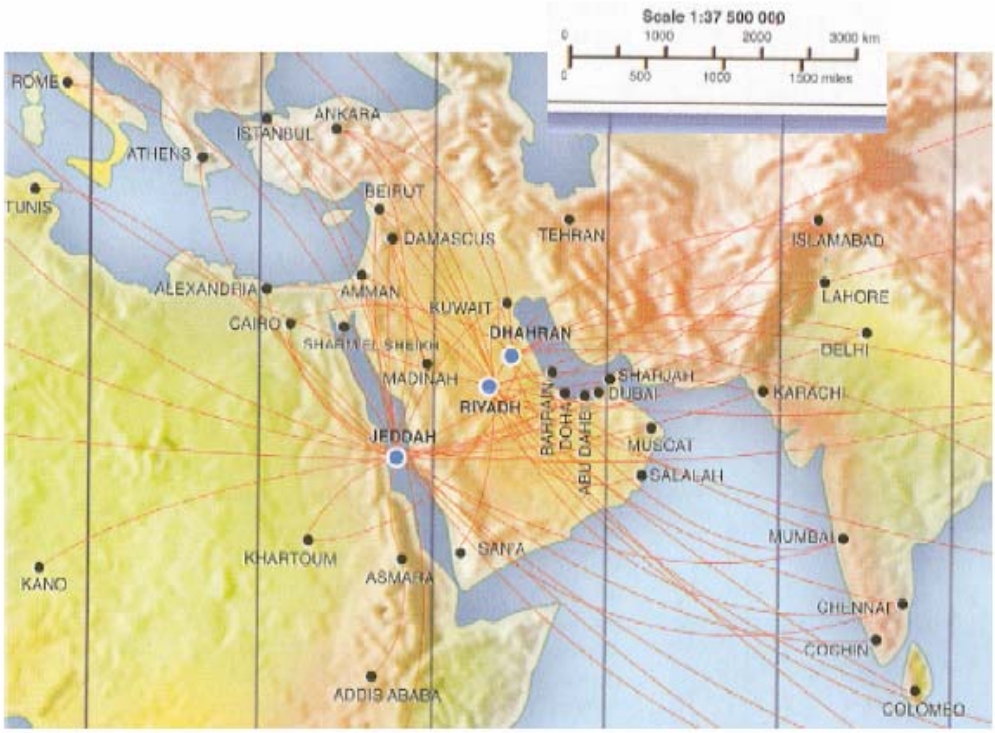

Regional Jets

Airplane Model	Price (millions US$)
MD-90	49.0 - 56.5
737-300	40.0 - 46.5

MD-90

Seating Capacity	18 F/C , 103 Y/C		
Length	152 ft 6 in		
Wingspan	107 ft 8 in		
Cruising speed	455 nmi/h	524 mi/h	$M = 0.80$
Maximum Cruising Altitude	37,000 ft		
Range	2,301 nmi/h	2,648 mi	

B737-268

Seating Capacity	14 F/C , 88 Y/C		
Length	100 ft 4 in		
Wingspan	93 ft		
Cruising speed	455 nmi/h	524 mi/h	$M = 0.79$
Maximum Cruising Altitude	35,000 ft		
Range	2,251 nmi	2,590 mi	

Figure 10.2 Regional Jets

10.3 Calculations of Our Aircraft:

These calculations were based on equations in the book and also assuming that Length of Certification Program is 7 years and the maintenance and operations are carried out every 1-year. This table shows the relevant information about the cost analysis of 1 aircraft.

Table 10.2 cost analyses of aircraft

Engineering Hours	208,670 hr
Tooling Hours	83,098 hr
Manufacturing Hours	42,802 hr
QC Hours (Quality and Control)	2,277 hr
Devel Support Cost	$6,212,906
Flight Test Cost	$1,011,818
Manufacturing Materials Cost	$308,790 /
Engineering Production Cost per Aircraft	$36,766,564
Cost of Avionics and Instruments	$110,000
RDT&E + flyaway	$36,766,564 per aircraft
O& M (Operation & Maintenance per year)	$1.5 M $ per aircraft

The Total Aircraft Price = RDT&E +flyaway + O&M costs
= 36.77 + 1.5 = 38.27 million $

10.3.1 Depreciation Consideration

Depreciation of aircraft for regular tax purposes for FAR Part 91 taxpayers is computed with a five-year life and a double declining balance method. Depreciation of aircraft for commercial operators for regular tax purposes is calculated under a seven-year life and a double declining balance method. For alternative minimum tax purposes the same useful lives are used, but the method is reduced from double declining balance to 150% declining balance .The new tax law excludes both the 30% bonus depreciation and the regular depreciation, on all new aircraft purchases, from the alternative minimum tax preference treatment. Simply stated, on new aircraft purchases the regular tax method will be used for both alternative minimum tax and regular tax.

Table 10.3 Depreciation over seven years

Year	New Aircraft Reg. & Alt. Min. Tax	Used Aircraft Regular Tax	Used Aircraft Alt. Min. Tax
1	44.0%	20.0%	15.0%
2	22.4 %	32.0%	25.5%
3	13.44%	19.2%	17.88%
4	8.06%	11.52%	16.66%
5	8.06%	11.52%	16.66%
6	4.03%	5.76%	8.33%

The Modified Accelerated Cost Recovery System (MACRS), is the allowable depreciation method to be used for aircraft placed in service after December 31,1986.

This model is used by aircraft companies or the owners of the private aircrafts assisting them to calculate the depreciation of their aircrafts.

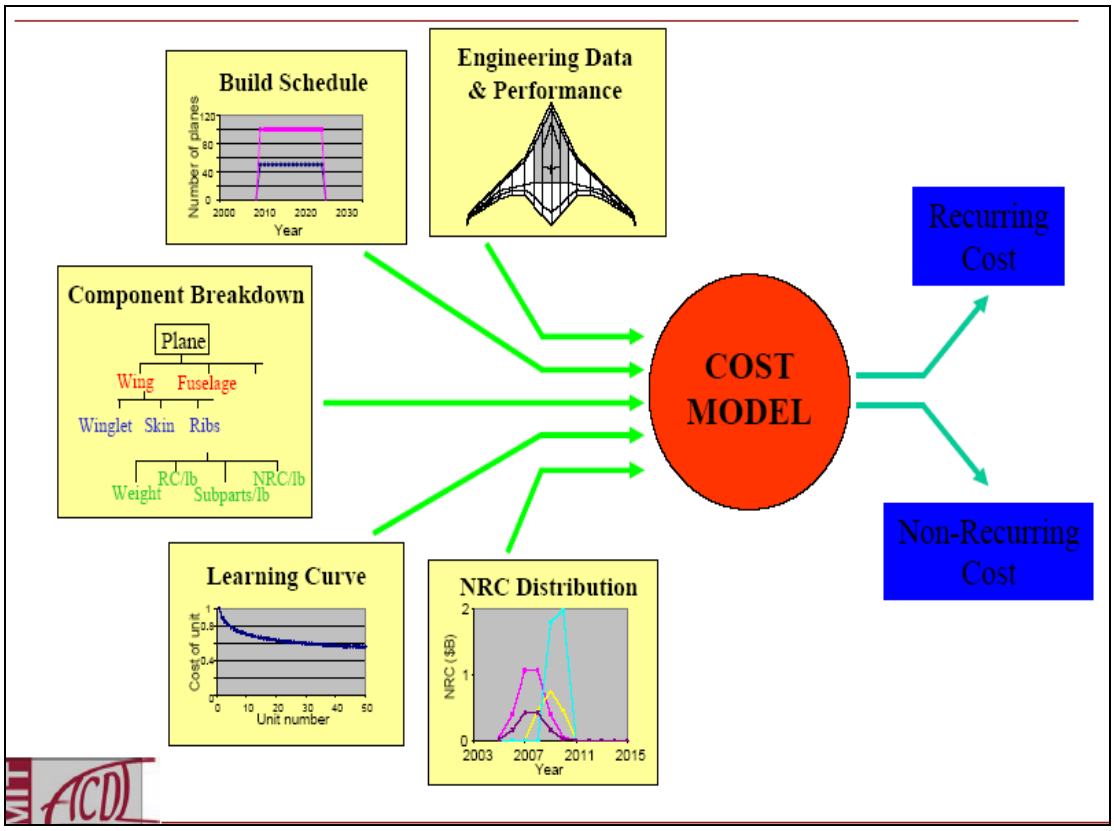

Figure 10.3 Cost Model Breakdowns

Conclusion:

The comparison with these existing two aircrafts in the market which are similar somehow to our aircraft, MD-90, which cruises at mach 0.8 and has a range of 2301 nm and the B737-268 which also cruises at mach 0.79 and has a range of 2251 nm shows that our 100 seat aircraft is much better and has three extra advantages. Our aircraft is cheaper than these two aircrafts and cost only 38.27 M$, plus that it has greater range for best performance of 4545 nm after conducting performance analysis as well as cruising faster than these existing aircrafts with mach 0.82.

11. Aircraft Final Layout

In the second part of this project, the processes were focused to improve the design of this aircraft as the usual manner in the aircraft conceptual design.

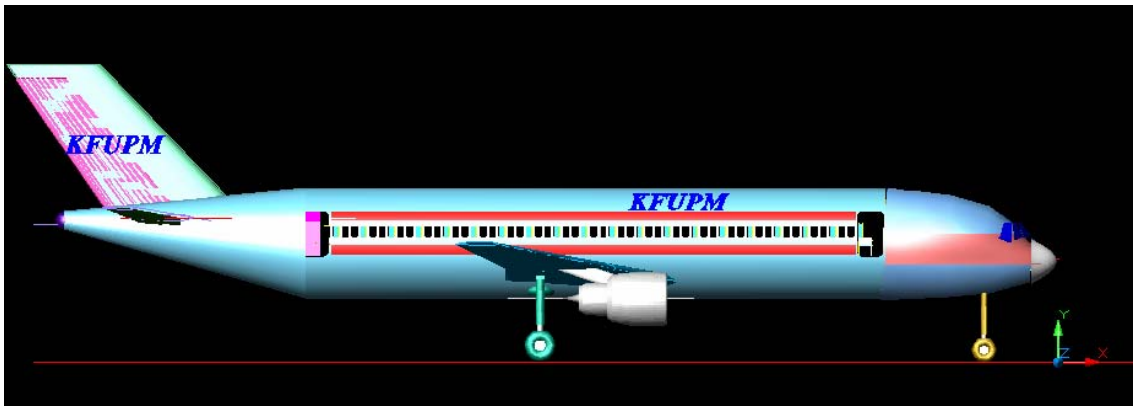

Figure 11.1 Aircraft Layout by using AutoCAD

11.1 Aircraft dimensions

After a lot of modifications on the aircraft initial design, the final design in this project came out with the following specifications:

Table 11.1 Fuselage shape

Fuselage shape	
Nose fineness	1.75
Tail fineness	2.5
Tail upsweep	15
Space for entry doors	50
Kitchen space	40" x 40"

Table 11.2 Wing geometry

Wing				
Area (Sref)	90.00	m^2	968.75	ft^2
Aspect ratio	8.60			
Taper ratio	0.27			
c/4 sweep	22.06	deg	0.39	radians
Dihedral	5	deg	0.09	radians
Span b	27.82	m	91.28	ft
le sweep	0.44	radians	25.27	deg
c, root	5.09	m	16.71	ft
c, tip	1.38	m	4.51	ft
MAC	3.591261235	m	11.78	ft
Ybar	5.622587592	m	18.45	ft
Wing ac	0.897815309	m	2.95	ft
Wing reference area	969.00	ft^2	90.02304576	m^2
Wing exposed area	783.00	ft^2	72.74308032	m^2
Airfoil t/c	0.10			
Wing wetted area	1552.06	ft^2	144.1913338	m^2

Table 11.3 Horizontal tail geometry

Horizontal tail				
c, root	9.39	ft	2.86	m
c, tip	3.52	ft	1.07	m
Span	36.52	ft	11.13	m
c/4 sweep	26.50	deg	0.46	radians
Dihedral	5.00	deg	0.09	radians
Area	235.74	ft^2	21.90064678	m^2
Aspect ratio	5.66			
Taper ratio	0.37			
le sweep	0.52	radians	30.07	deg
HT MAC	6.899834753	ft	2.10	m
HT Ybar	7.746238058	ft	2.36	m
Tail ac	1.724958688	ft	0.53	m
Sh/S	0.243			
cHT	1.00			
Tail arm LHT (calculated)	48.42	ft	14.76	m
Tail arm LHT (as-drawn)	47.75	ft	14.55	m

Table 11.4 Vertical tail geometry

Vertical tail				
c, root	14.36	ft	4.38	m
c, tip	10.19	ft	3.11	m
Height	15.42	ft	4.70	m
c/4 sweep	39.31	deg	0.69	radians
Dihedral	0.00	deg	0.00	radians
Area	189.28	ft^2	17.58473386	m^2
Aspect ratio	1.26			
Taper ratio	0.71			
le sweep	0.76	radians	43.65	deg
VT MAC	12.39305092	ft	3.78	m
VT Ybar	3.636733198	ft	1.11	m
Tail ac	3.098262729	ft	0.94	m
Sv/S	0.195			
cVT	0.09			
Tail arm LVT (calculated)	42.04	ft	12.82	m
Tail arm LVT (as-drawn)	54.32	ft	16.56	m

Table 11.5 Landing Gear dimensions

Landing Gear				
Wheelbase	54.9	ft	16.73352	m
Wheel track	25	ft	7.62	m
Main LG height (ground)	9	ft	2.7432	m
Main LG height (air)	12	ft	3.6576	m

Table 11.6 Aircraft Fuel Tanks

Fuel Tanks		
Total fuel volume	385	cu. ft.
Fuel volume in wings	256	cu. ft.
Fuel volume aft of cg	78	cu. ft.
Fuel volume fore of cg	78	cu. ft.

11.2. The cross-section of the aircraft

It's the same one in the initial layout. The aircraft can carry 100 passengers, the following requirements for the cross section are shown in table (5.1)

Table 11.7 Aircraft Cross Section

Seat pitch	0.9144	m
Seat width	0.4572	m
Headroom	1.6002	m
Seat layout	3-0-2	
Number of seats	100	
No. of seat rows	20	

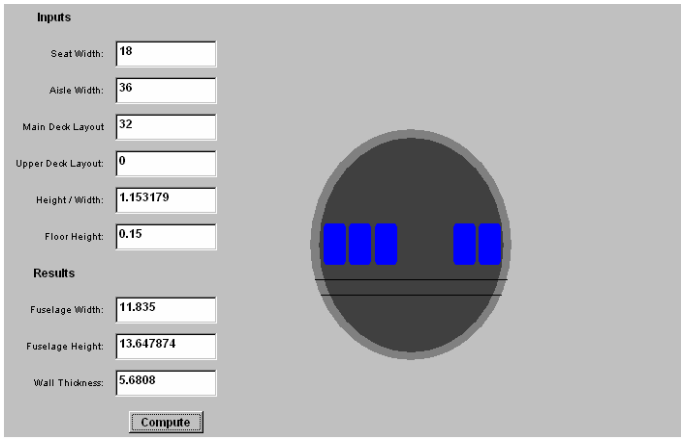

Figure 11.2 Aircraft Cross Section by using the Java applet

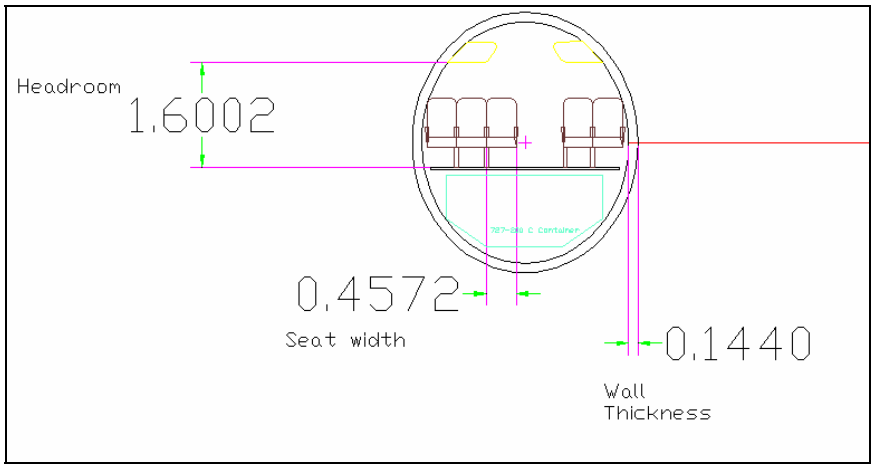

Figure 11.3 Aircraft Cross Section by using AutoCAD

11.3. The Top View of Aircraft:

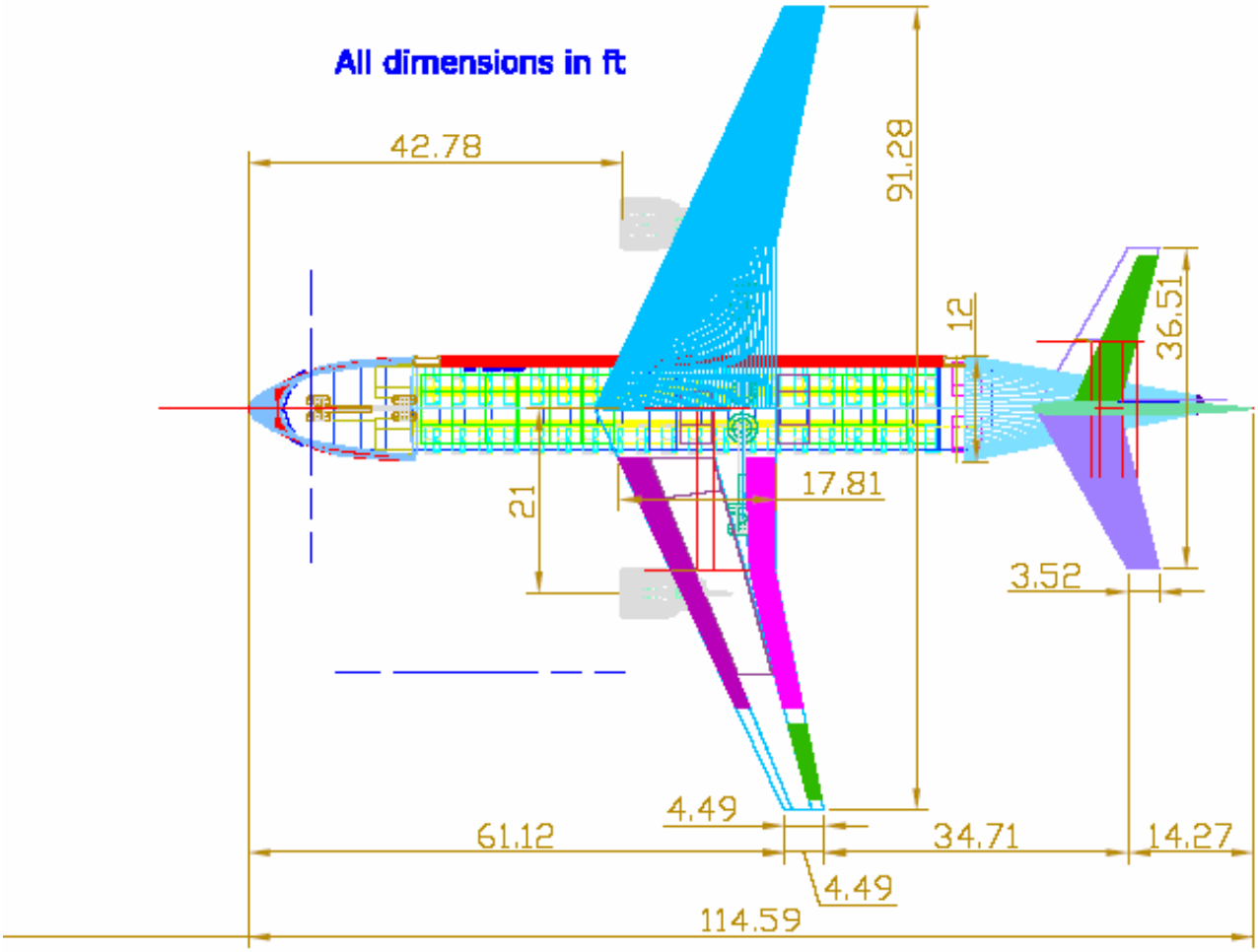

Figure 11.4 The Top View of the Final Layout

11.4. The Side view:

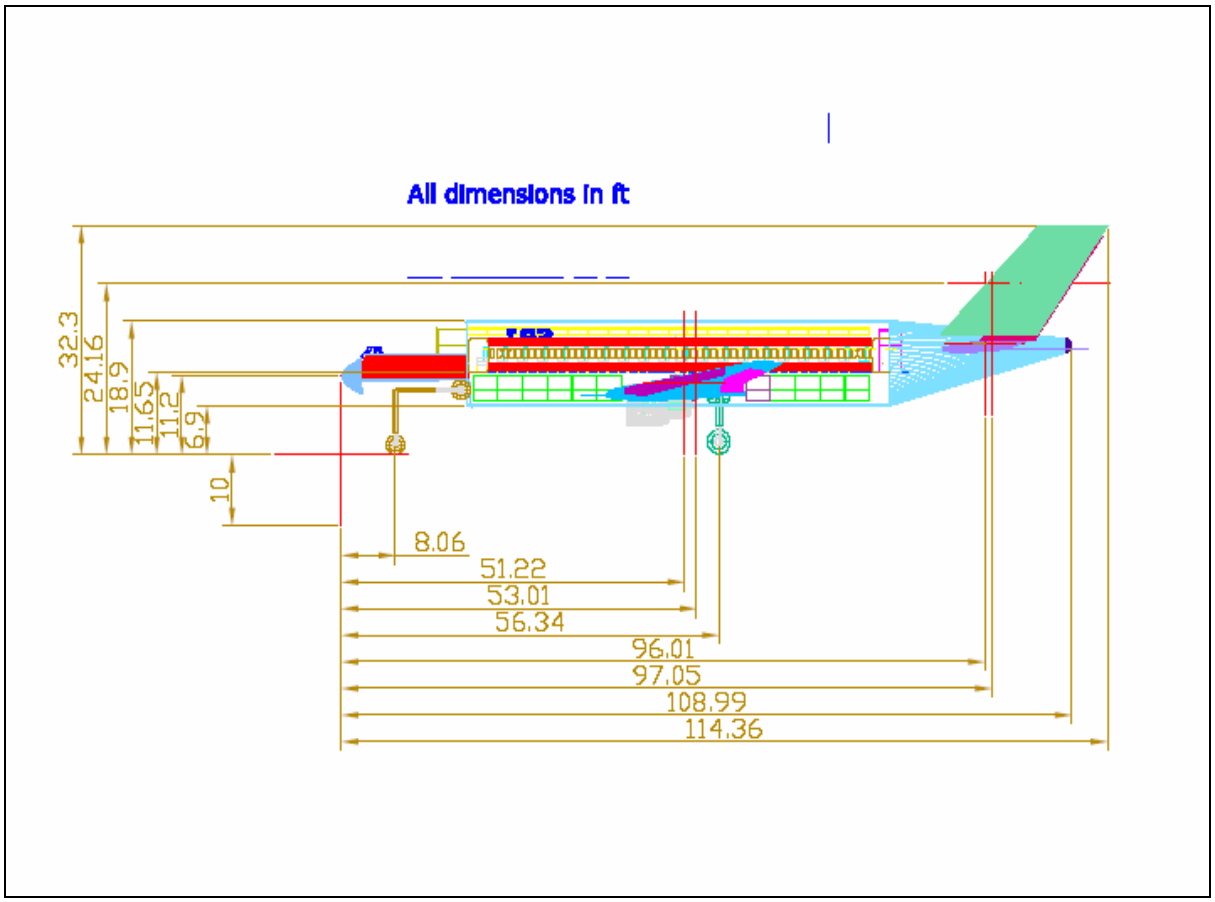

Figure 11.5 The Side View of the final layout with some basic dimensions

11.5. The Front View

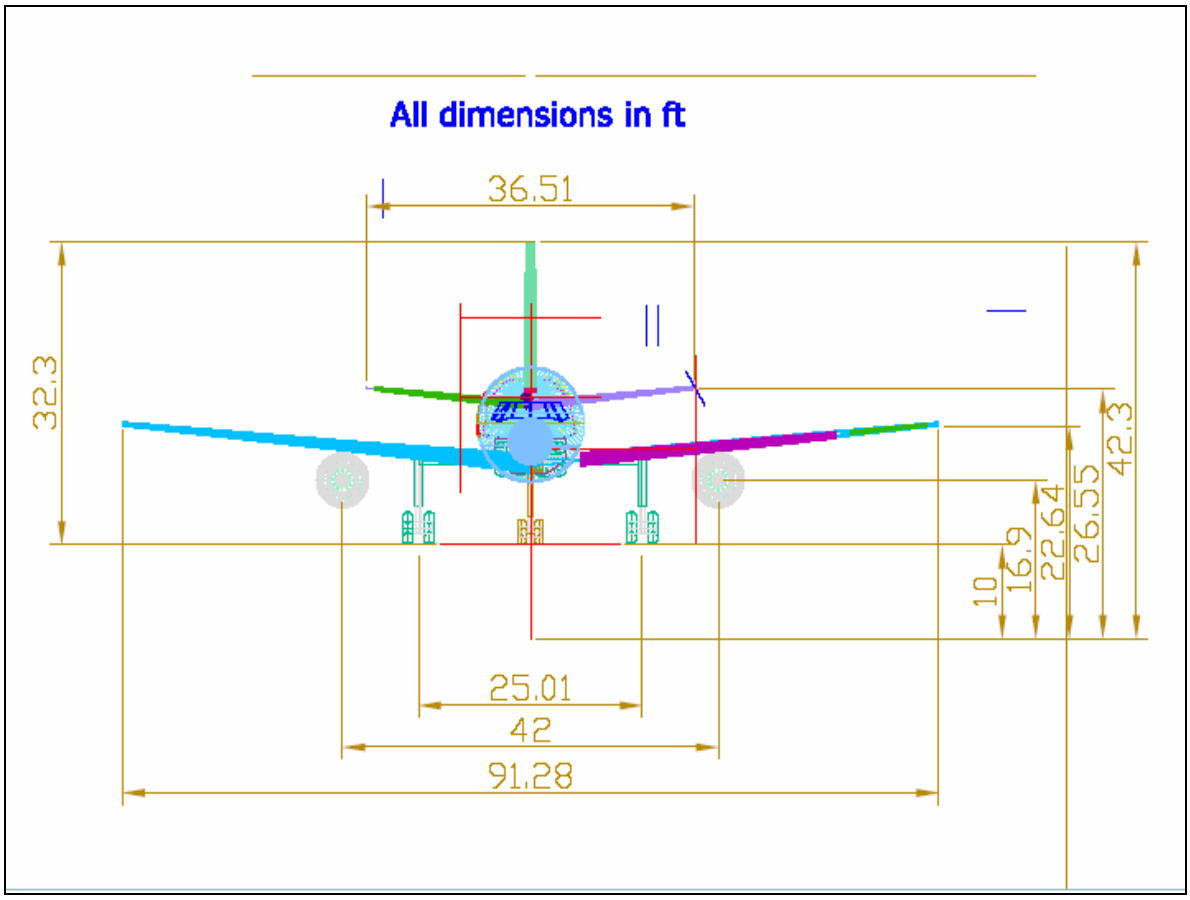

Figure 11.6 The Front View of the final layout with some basic dimensions

From figure (5.14),

- The wing span = 91.28 ft =27.82m.
- The horizontal tail span =36.51 ft =11.13m.

11.6. Some Basic Dimensions:

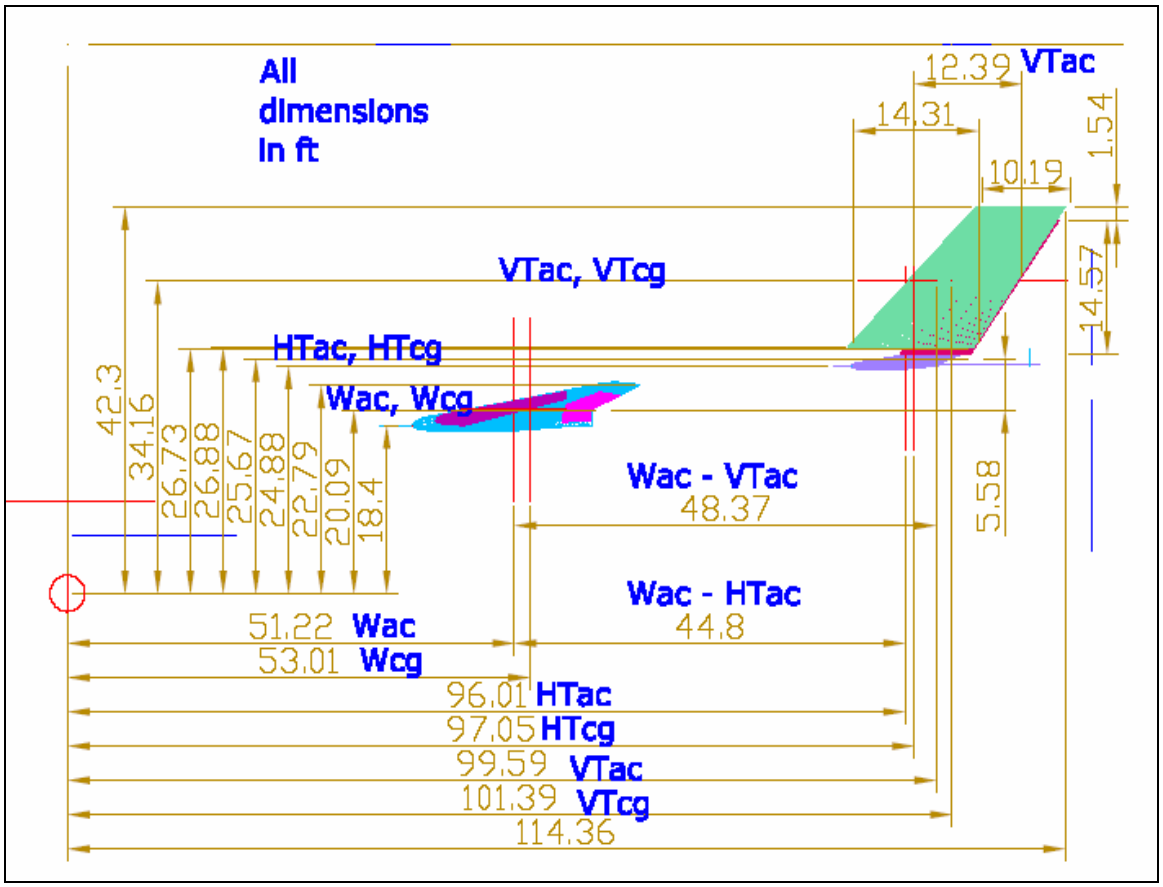

Figure 5.15 Some basic dimensions of the final layout

12. Conclusion

The objective of this project was to design an 80-100 seat commuter aircraft capable of transporting passengers and baggage along principal air routes within the Kingdom and the Gulf region with minimizing direct operating costs and cost per passenger miles in terms of fuel consumption, simplifying maintenance operations while incorporating advanced technology in airframe and engine designs. Taking care that the aircraft satisfy FAA regulations. With the following chrematistics:

- Mission Profile
  – Warm Up/Taxi for 10 min, sea level, standard day.
  – Take off within distance specified in Special
  – Climb at best rate of climb to cruising altitude of 36,000 ft.
  – Cruise at *V* best range (knots) for best range (nm).
  – Land with reserve fuel for additional 100 nm range and 20 min loiter at 5000 ft.
  – Taxi to gate for 10 min, sea level, standard day 30 c^o.

- Special Design Requirements
  – Takeoff Distance (FAR 25 Balanced field length)
    • Concrete: sea level standard day < 5000 ft. at max TOGW
  – Climb Performance:
    • Two engine sea level standard day climb rate > 2100 fpm
  – Cruise Performance:
    • Best range velocity V of 0.8 Mach number for best range of 1500 nm or more and greater than 300 kts true airspeed at 36,000 ft.

Progressing in this design project was by following exactly step by step the aircraft design techniques in Raymer's book (aircraft design: A conceptual Approach).
Everybody of the team was doing specific task and there was distribution of results and till writing this report by the leader.

In this project all requirements were satisfied according as it was stated in the problem statement. This aircraft is willing to be in service since it has good flying qualities economic and fast aircraft. It has range e of 4545 nm after performing performance analysis for best cruise conditions, it flies at Mach 0.8, it costs about 38.72 M$ and some advanced technology was applied by using winglets and composite materials.

After looking to the market survey that was carried on similar aircraft that are similar to our designed one and that are used by Saudia Airlines, MD-90 and B737-268 designed. It was found that comparison with these two existing aircraft that the MD-90 aircraft that cruises at Mach 0.8 and has a range of 2301 nm and the B737-268 that cruises at Mach

0.79 and has a range of 2251 nm shows that our 100 seat aircraft is much better and has three extra advantages. Our aircraft is cheaper than theses two aircrafts and costs only 38.27 M$, plus that it has greater range for best performance of 4545 nm after conducting performance analysis, as well as cruising faster than these aircrafts with mach 0.82. To conclude, our aircraft is highly recommended to be considered and worth buying.

References

1. “Regional market outlook 2001” Bombardier Aerospace, Montreal, Canada, 2001.

2. News except from Arab Airlines Organization at www.aaco.org, 2004.

3. “Ahlan Wasahlan,” In flight magazine of Saudi Arabian Airlines, may 2004.

4. Raymer, D. P., “Aircarft Design: A conceptual Aprroach,” AIAA Education Series, 1989.

5. Stanford Univerwsity Aircraft Design Course (text and java programs) at http://adg.stanford.edu/aa241/aircraftdesign.html.

6. http://raphael.mit.edu/xfoil/

7. http://www.nada.kth.se/~chris/pablo/pablo.html

8. http://www.pagendarm.de/

Appendences

Appendix A (Propulsion AND fuel System):

Manufacturer	BAe	BAe	BAe	TUPOLEV	TUPOLEV	DOUG.	DOUG.	BOEING	BOMB.	
Type								717-	CRJ	
Model	RJ70	RJ85	RJ100	Tu-134	Tu-334	DC 9-10	DC 9-30	200	900	Average
Engine Manufacturer	Textron	Textron	Textron	Soloviev	Lotarev	PW	PW	BMW R-R	GE	
Model / Type	LF507	LF507	LF507	D-30 Srs II	D-436T1	JT8D-5	JT8D-7	715	CF34-8C5	
No. of engines	4	4	4	2	2	2	2	2	2	24.00
Static Thrust (kN)	27.3	31.1	31.1	66.7	73.6	54.5	62	97.9	58.4	49.35

Table A.1 Average Data

A.4-2 High-bypass turbofan characteristics

Sea-level static thrust, lb	50,000
Sea-level static TSFC, 1/hr	0.40
Sea-level static airflow, lb/s	1,680
Bare-engine weight, lb	7,700
Engine length, in.	150
Maximum engine diameter, in.	100
Overall pressure ratio	30
Fan pressure ratio	1.6
Bypass ratio	8.0

Table A.2 Turbofan Characteristics

Engine Performance Curves:

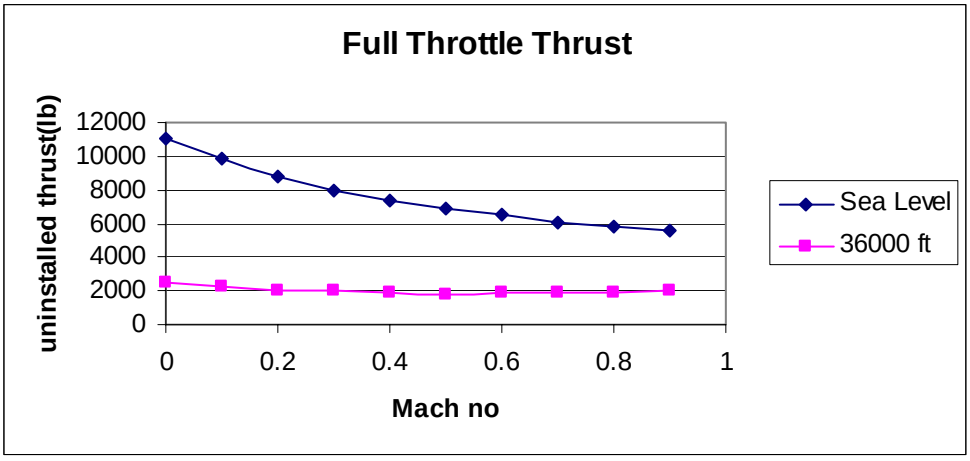

Figure A.1 Full Throttle Thrust

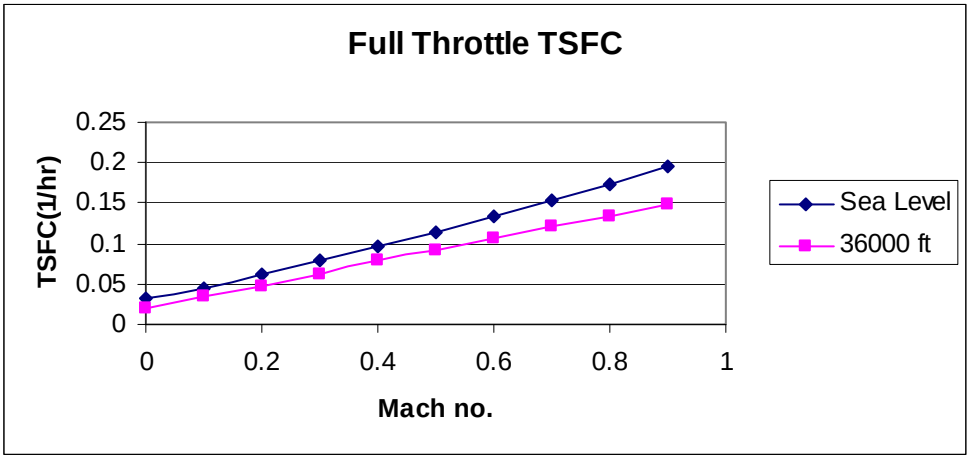

Figure A.2 Full Throttle Thrust

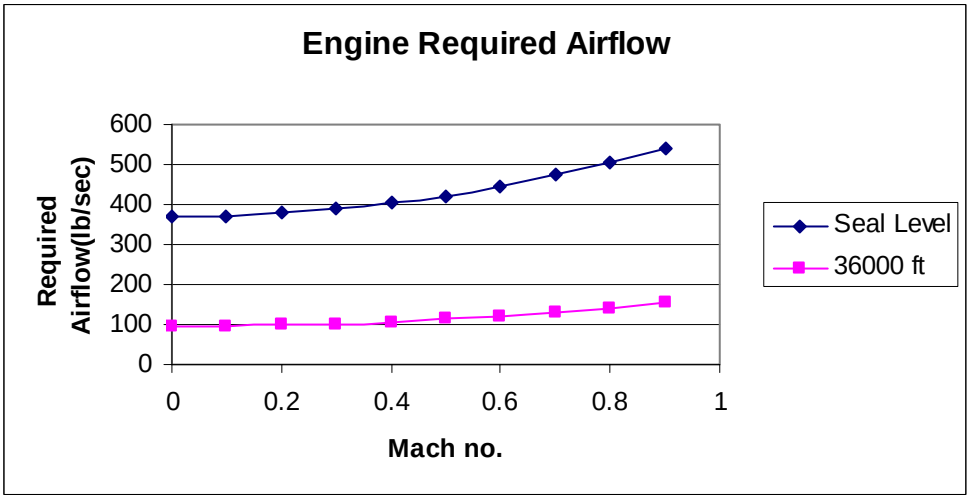

Figure A.3 Engine Required Airflow

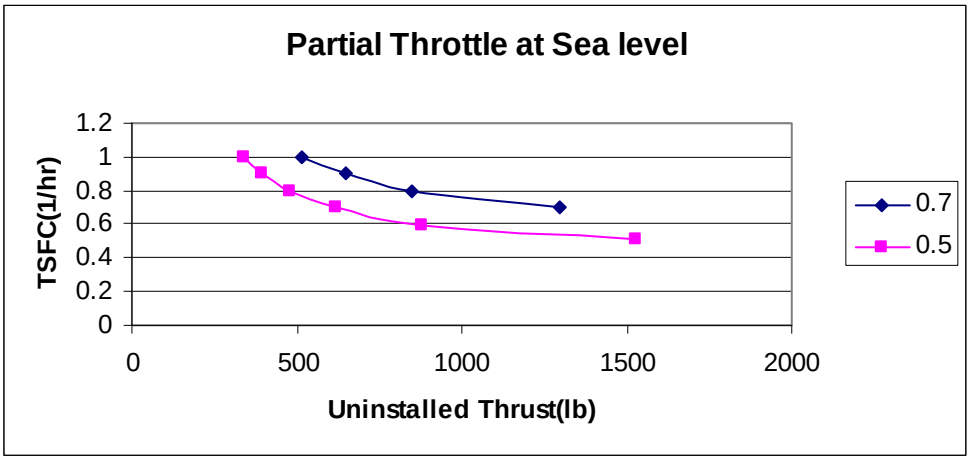

Figure A.4 Partial Throttle at Sea Level

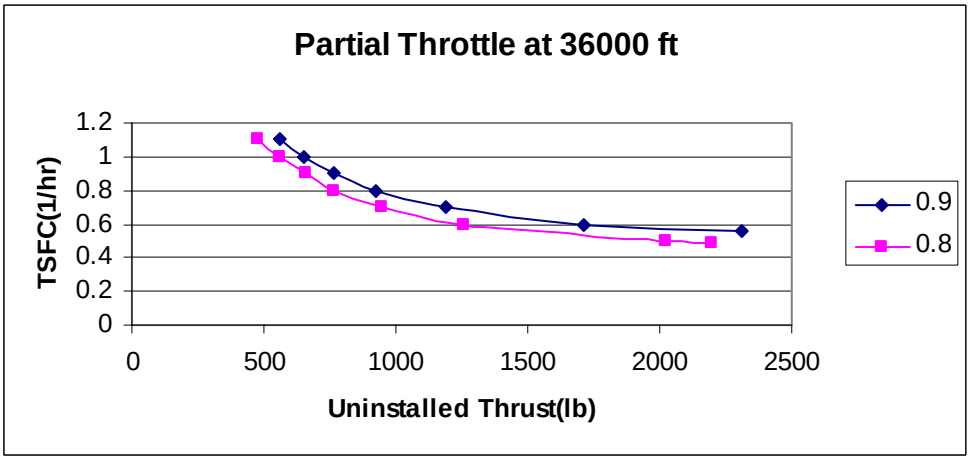

Figure A.5 Partial Throttle at 36,000 ft

fueslage segment	cross sec-area of fuel tank				fueslage	fueslage
	fuel tank #1	fuel tank #2	fuel tank #3	fuel tank #4	area	area
0.000	0.000	0.000	0.000	0.000	1.340	0.000
1.000	0.000	0.000	0.000	0.000	2.102	0.000
2.000	0.000	0.000	0.000	0.000	2.582	0.000
3.000	0.000	0.000	0.000	0.000	2.920	0.000
4.000	0.000	0.000	0.000	0.000	3.161	0.000
5.000	0.000	0.000	0.000	0.000	3.161	0.000
6.000	0.000	0.000	0.000	0.000	3.161	0.000
7.000	0.000	0.000	0.000	0.000	3.161	0.000
8.000	0.000	0.000	0.000	0.000	3.161	0.000
9.000	0.000	0.000	0.000	0.000	3.161	0.000
10.000	0.000	0.000	0.000	0.000	3.161	0.000
11.000	0.000	0.000	0.000	0.000	3.161	0.000
12.000	0.000	0.000	0.000	0.000	3.161	0.006
13.000	0.619	0.147	0.147	0.000	3.161	0.620
14.000	0.184	0.864	0.864	0.000	3.161	2.263
15.000	0.000	0.718	0.718	0.000	3.161	3.144
16.000	0.000	0.000	0.000	0.000	3.161	4.265
17.000	0.000	0.000	0.000	0.666	3.161	6.544
18.000	0.000	0.000	0.000	0.136	3.161	7.451
19.000	0.000	0.000	0.000	0.000	3.161	3.700
20.000	0.000	0.000	0.000	0.000	3.161	1.438
21.000	0.000	0.000	0.000	0.000	3.161	0.298
22.000	0.000	0.000	0.000	0.000	3.161	0.000
23.000	0.000	0.000	0.000	0.000	3.161	0.000
24.000	0.000	0.000	0.000	0.000	3.161	0.000
25.000	0.000	0.000	0.000	0.000	3.161	0.000
26.000	0.000	0.000	0.000	0.000	3.161	0.000
27.000	0.000	0.000	0.000	0.000	3.161	0.000
28.000	0.000	0.000	0.000	0.000	3.161	0.000
29.000	0.000	0.000	0.000	0.000	3.161	0.000
30.000	0.000	0.000	0.000	0.000	3.021	0.000
31.000	0.000	0.000	0.000	0.000	0.845	0.000
32.000	0.000	0.000	0.000	0.000	0.454	0.000
33.000	0.000	0.000	0.000	0.000	0.032	0.000
34.000	0.000	0.000	0.000	0.000	0.000	0.000

Table (4.3): Area and Fuel Volume Distribution

Appendix B (Aerodynamics)

B.1 Aircraft Dimensions

Found at [http://webcourses.kfupm.edu.sa/SCRIPT/AE427/scripts/serve_home]

B.2 Useful variables (Mat lab program)

```
% K & e
AR=8.6;
e=(4.61*(1-(0.045*AR^.68)*(cos(0.44)))^.15)-3.1
K=1/(pi*AR*e)
% e =1.3782 & K =0.0269

% Kh & eh
AR=5.66
e=(4.61*(1-(0.045*AR^.68)*(cos(0.44)))^.15)-3.1
K=1/(pi*AR*e)
% e=1.4129 & K=0.0398


% Re=den*M*a*MAC/visc
den=0.0008907;M=0.82;a=994.8;MAC=11.78;visc=0.311e-
6;
Re=den*M*a*MAC/visc
% Re = 2.7521e+007
```

B.3 wing coefficients (Excel)

Alpha	Cl	Cm	Cd		Cd	Cl
-1	0.31	-0.105	0.006		0.006	0.31
-0.5	0.43	-0.103	0.006		0.006	0.43
0	0.55	-0.101	0.006		0.006	0.55
0.5	0.67	-0.1	0.006		0.006	0.67
1	0.8	-0.098	0.006		0.006	0.8
1.5	0.93	-0.095	0.006		0.006	0.93
2	1.06	-0.091	0.006		0.006	1.06
2.5	1.21	-0.085	0.006		0.006	1.21
3	1.36	-0.077	0.006		0.006	1.36
3.5	1.54	-0.066	0.006		0.006	1.54
4	1.73	-0.049	0.007		0.007	1.73
4.5	1.97	-0.024	0.007		0.007	1.97
5	2.29	0.017	0.007		0.007	2.29
5.5	2.82	0.108	0.007		0.007	2.82
6	3.28	0.177	0.007		0.007	3.28
6.5	2.93	0.055	0.007		0.007	2.93

B.4 3-D lift coefficients for wing (Mat lab Program)

```
% WING CL(Alpha):
% CL_Alpha=[aa/2+sqrt(4+bb*(1+cc)]*(Sexp/Sref)*F
AR=8.6;
aa=2*pi*AR;
M=0.82;Eta=0.95;
Beta=sqrt(1-M^2);
bb=AR^2*Beta^2/Eta^2;
cc=(tan(.3665))^2/(Beta)^2;
Sexp=783;Sref=969;d=12;b=91.28;
F=1.07*(1+(d/b))^2;
CL_Alpha=(aa/(2+sqrt(4+bb*(1+cc))))*(Sexp/Sref)*F
% CL(ALpha) =  6.9943/rad = 0.1221/deg

% WING CL(max):
% CLmax=0.9*Clmax*cos(0.39)
Clmax=3.28;
CLmax=0.9*Clmax*cos(0.39)
 % CL(max) = 2.7303
```

B.5 H-Tail coefficients (Excel)

Alpha	Cl	Cm	Cd	Cd	Cl
0	0	0	0.005	0.005	0
1	0.1184	-0.0007	0.005	0.005	0.1184
2	0.2367	-0.0014	0.0051	0.0051	0.2367
3	0.3544	-0.002	0.0051	0.0051	0.3544
4	0.4713	-0.0027	0.0052	0.0052	0.4713
5	0.5873	-0.0033	0.0053	0.0053	0.5873
6	0.702	-0.0039	0.0056	0.0056	0.702
7	0.8152	-0.0046	0.0059	0.0059	0.8152
8	0.9267	-0.0052	0.0063	0.0063	0.9267
9	1.0363	-0.0058	0.0069	0.0069	1.0363
10	1.1436	-0.0064	0.007	0.007	1.1436
11	1.2485	-0.0071	-282.633	-282.633	1.2485

B.6 3-D H-Tail coefficient (Mat lab program)

```
% TAIL CL(ALpha):
 % CL_Alpha=[aa/2+sqrt(4+bb*(1+cc)]*(Sexp/Sref)*F
 AR=5.66;
aa=2*pi*AR;
M=0.82;Eta=0.95;
Beta=sqrt(1-M^2);
bb=AR^2*Beta^2/Eta^2;
cc=(tan(.4))^2/(Beta)^2;
Sexp=190.2690;Sref=235.467;d=12;b=36.52;
F=1.07*(1+(d/b))^2;
CL_Alpha=(aa/(2+sqrt(4+bb*(1+cc))))*(Sexp/Sref)*F
% CL(Alpha) = 8.1157/rad =  0.1416/deg

% Tail CL(max):
% CLmax=0.9*Clmax*cos(0.46)
Clmax=1.1436;
CLmax=0.9*Clmax*cos(0.46)
 % CL(max) =  0.9223
```

B.7 Drag coefficient (Mat lab program)

```
% WING:
% CD=CD_min+K(CL-CL_mindrag)^2
CD_min=0.006;K=0.0269;CL=0.9*2.7359;CL_mindrag=0.31;
CD=CD_min+K*(CL-CL_mindrag)^2
% CD = 0.1306

% H-TAIL:
% CD=CD0+KCL^2
CD0=0.005;K=0.0398;CL=0.9*0.9223;
CD=CD0+K*CL^2
% CD = 0.0324
```

B.8 CL & CD varies with flap hinge angle (Excel)

FlabDef	Clmax
0	0.8296
1	0.845
2	0.86
3	0.875
4	0.89
5	0.9
6	0.92
7	0.93
8	0.95
9	0.96
10	0.97
11	0.99
12	1
13	1.01
14	1.02
15	1.04

FlabDef	CD0
0	0
1	0.001357
2	0.002714
3	0.004071
4	0.005428
5	0.006785
6	0.008142
7	0.009499
8	0.010856
9	0.012213
10	0.01357
11	0.014927
12	0.016284
13	0.017641
14	0.018998
15	0.020355

CD0	Clmax
0	0.8296
0.001357	0.845
0.002714	0.86
0.004071	0.875
0.005428	0.89
0.006785	0.9
0.008142	0.92
0.009499	0.93
0.010856	0.95
0.012213	0.96
0.01357	0.97
0.014927	0.99
0.016284	1
0.017641	1.01
0.018998	1.02
0.020355	1.04